frontiers in Immunology

TYPE Original Research
PUBLISHED 02 November 2026
DOI 10.3389/fimmu.2026.1885356

Check for updates

OPEN ACCESS

EDITED BY
Penghua Wang,
UCONN Health, United States

REVIEWED BY
Duomeng Yang,
Jinan University, China
Mohsen Sharif-zak,
Shahid Beheshti University of Medical Sciences, Iran

*CORRESPONDENCE
Jan Frič
jan.fric@fnusa.cz

†These authors share first authorship

RECEIVED 19 May 2026
REVISED 02 October 2026
ACCEPTED 14 October 2026
PUBLISHED 02 November 2026

CITATION
Papatheodorou I, Lázničková P, Feglarová T, Blažková G, Kuglerová K, Santocki M, Jurásková M, Kafka F, Kolovos P, Vojtišek L, Radvan M, Bartys P, Ulčák D, Rektorová I, Hortová Kohoutková M, Bartečková E and Frič J (2026) Persistent neutrophil maturation deficits associate with cognitive impairment in individuals with post-acute sequelae of COVID-19. *Front. Immunol.* 17:1885356. doi: 10.3389/fimmu.2026.1885356

COPYRIGHT
© 2026 Papatheodorou, Lázničková, Feglarová, Blažková, Kuglerová, Santocki, Jurásková, Kafka, Kolovos, Vojtišek, Radvan, Bartys, Ulčák, Rektorová, Hortová Kohoutková, Bartečková and Frič. This is an open-access article distributed under the terms of the Creative Commons Attribution License (CC BY). The use, distribution or reproduction in other forums is permitted, provided the original author(s) and the copyright owner(s) are credited and that the original publication in this journal is cited, in accordance with accepted academic practice. No use, distribution or reproduction is permitted which does not comply with these terms.

Persistent neutrophil maturation deficits associate with cognitive impairment in individuals with post-acute sequelae of COVID-19

Ioanna Papatheodorou[1,2†], Petra Lázničková[1,3†], Tereza Feglarová[4], Gabriela Blažková[1,2], Kateřina Kuglerová[4], Michal Santocki[1], Martina Jurásková[1,3], Filip Kafka[1,2], Petros Kolovos[5], Lubomír Vojtišek[6], Martin Radvan[7], Patrik Bartys[8], David Ulčák[6,9], Irena Rektorová[6,9], Marcela Hortová Kohoutková[1,3], Eliška Bartečková[8] and Jan Frič[1,3,4*]

[1]Cellular & Molecular Immunoregulation Group, International Clinical Research Center (ICRC), St. Anne's University Hospital, Brno, Czechia, [2]Department of Biology, Faculty of Medicine, Masaryk University, Brno, Czechia, [3]International Clinical Research Center (ICRC), Faculty of Medicine, Masaryk University, Brno, Czechia, [4]Institute of Hematology and Blood Transfusion, Prague, Czechia, [5]Department of Molecular Biology and Genetics, Democritus University of Thrace, Alexandroupolis, Greece, [6]Brain and Mind Research Program, Central European Institute of Technology, Masaryk University, Brno, Czechia, [7]Department of Internal Medicine and Cardiology, University Hospital Brno and Faculty of Medicine of Masaryk University, Brno, Czechia, [8]Department of Psychiatry, Faculty of Medicine, Masaryk University and University Hospital Brno, Brno, Czechia, [9]First Department of Neurology, Faculty of Medicine, Masaryk University and St. Anne's University Hospital, Brno, Czechia

Introduction: Post-COVID-19 condition, or post-acute sequelae of COVID-19 (PASC), is characterized by persistent cognitive impairments and immune dysregulation. While neutrophils are critical in acute COVID-19, whether their long-term functional dysregulation contributes to PASC, remains unclear. Thus, we investigated the links between immune system changes, symptom severity and cognitive impairment in PASC.

Methods: In this cross-sectional study, we enrolled 40 individuals with self-reported issues with COVID-19 recovery (PASC) and 37 fully recovered (REC) volunteers. Participants were post-infection at either TP1 (from 6 up to 18 months post-infection, 7 PASC, 20 REC) or at TP2 (from 19 up to 36 months post-infection, 33 PASC, 17 REC). We evaluated the Newcastle post-COVID-19 Syndrome Follow Up Screening (NC) scores for symptom severity, and neuropsychological tests for memory, attention, and executive function. Peripheral blood was analyzed using multicolor flow cytometry, ELISA, clustering, and multivariate regression.

Results: PASC participants in both the TP1 cohort and the TP2 cohort, demonstrated increased NC scores and significant changes in neutrophil numbers and subset composition. In the TP1 cohort, the PASC group showed an increased frequency of activated $CD16^{+}CD62L^{low}$ neutrophils and a reduced frequency of $CXCR4^{+}TREM\text{-}1^{+}CCR2^{+}$ polymorphonuclear myeloid-derived suppressor cells (PMN-MDSCs). This was accompanied by elevated soluble TNF receptor 1 (sTNFR1) and decreased sTNFR2 and CXCL12. In the TP2 cohort,

PMN-MDSC levels were comparable between REC and PASC groups, alongside increased emergency granulopoiesis regulators IL-3 and IL-6. Multivariate regression revealed significant associations between PMN-MDSC signatures, granulopoiesis-related markers, NC scores, and cognitive test scores in either the TP1 or the TP2 cohort. These results represent cross-sectional observations in participants assessed within the respective post-infection intervals, rather than longitudinal evidence of persistence. The results show that dysregulated granulopoiesis and neutrophil maturation are present even at 18 and 36 months in PASC individuals, potentially associating with overall symptom severity and cognitive impairment.

Conclusions: Despite limitations in cohort size, requiring validation of the associations in larger cohorts, our findings may contribute to the further understanding of PASC and future new transitional perspectives for PASC management.

KEYWORDS

biomarkers, cognitive decline, immune dysregulation, neutrophils, PASC, PMN-MDSC, post-acute COVID sequelae, SARS-CoV-2

1 Introduction

Post-COVID-19 condition, also known as long-COVID, or post-acute sequelae of COVID-19 (PASC) has affected up to 35% individuals after SARS-CoV-2 infection, in non-vaccinated individuals during the years 2020–2021 of the pandemic, and the first trimester of 2022 (Wild-type, Alpha, and Delta waves). Even though widespread vaccination and the milder Omicron variant have led to a reduction of this percentage, PASC still persists in 10-20% of COVID patients (1–3), manifesting as multisystem disturbances such as fatigue, respiratory compromise, myalgia, sensory deficits, gastrointestinal issues, and cognitive impairments. Cognitive impairments are, along with fatigue, amongst the most common symptoms of PASC, and involve deficits in learning and memory, executive and perceptual motor function, complex attention and language skills (4–8). However, the pathogenesis of PASC is currently unknown, and there are therefore no targeted treatments. Additionally, the heterogeneity of symptomσ and the attribution of some symptoms to other conditions, further hinders the detection and management of PASC.

The immune and neuropathological aspects are both important and seem interconnected in PASC. Several neuropathological processes initiated during acute COVID-19, such as systemic inflammation and endothelial activation during COVID-19 which disrupt the blood–brain barrier (BBB), may contribute to the development of long-term cognitive symptoms observed in PASC. These processes have been associated with microglial overactivation, white matter demyelination, brainstem abnormalities, elevated inflammatory markers and neuroinflammatory changes, which may be associated with increased disease severity, and poorer functional recovery (9–11). Elevated neuroinflammation markers and brain metabolic impairment have also been linked to persistent cognitive symptoms in the weeks following infection (12–16). These alterations coincide with immune dysregulation during both acute and post-acute phases of COVID-19. Elevated acute-phase proteins and proinflammatory cytokines following infection correlate with microglial dysfunction and neuroinflammation (9, 16). Additionally, increased formation of neutrophil extracellular traps (NETs), accumulation of senescent T cells, elevated soluble TNF receptors (sTNFR1, sTNFR2), and other inflammatory mediators such as TNF-α, IL-1β, IL-10, IL-6, CXCL8, and immune senescence markers have all been observed in post-acute COVID-19 (16–18). Although these inflammatory profiles can be associated with PASC symptoms (12), these processes have largely been examined in isolation, rather than as interconnected mechanisms, limiting our ability to fully understand how immune dysregulation may drive persistent symptoms in PASC and hindering diagnostic processes.

Among the immune pathways implicated in neuroinflammation, neutrophils are of particular interest due to their prominent role in acute COVID-19 and their potential to mediate long-term inflammatory effects. In acute COVID-19 neutrophils drive early inflammation through phagocytosis, degranulation, proinflammatory cytokine release, and NET formation., these functions correlate with disease severity, microvascular thrombosis, systemic inflammation, and tissue injury. More importantly neutrophils contribute to chronic inflammation (18–20), as they remain hyperactivated for months after infection, exhibiting persistent functional dysregulation indicative of a role in chronic inflammation (18, 20–22). In parallel, pathologically activated subsets, including immature immunosuppressive polymorphonuclear myeloid-derived suppressor cells (PMN-MDSCs), generated via emergency granulopoiesis, expand during acute disease and associate with higher pro-inflammatory cytokine production, worse prognosis, more severe acute disease and higher mortality (21, 23–26). These immature subsets may also persist for months after viral clearance, and are associated with long-term immunosuppression and higher number of reported symptoms, 3 months after infection (21, 23, 24). Consequently, persistent dysregulation of neutrophil maturation may drive long-term PASC-related cognitive deficits. However, functional neutrophil data beyond 12 months post-infection remain limited and thus their role in long-term PASC development remains unexplored.

In this study, we determined immune alterations in fully recovered vs PASC-reporting individuals with unbiased clustering.

TABLE 1 Demographic and clinical characteristics of the patients enrolled in the study.

Study group	REC		PASC	
Timepoint	TP1	TP2	TP1	TP2
Number of participants (n)	20	17	7	33
Sex (male/female), n (%)	7 (35.0)/ 13 (65.0)	11 (64.7)/ 6 (35.3)	4 (57.1)/ 3 (42.9)	13 (39.4)/ 20 (60.6)
Age, median [IQR]	41 [38-46]	39 [34.25-46.5]	45 [41.5-54.5]	46 [38-55.5]
BMI, median [IQR]	25.1 [23.7-27.8]	27.8 [23.8-31.4]	27.8 [25.4-30.2]	27.4 [25.3-32.5]

Data regarding patient age and BMI are presented as median (+/- interquartile range; IQR).

Neutrophil subsets demonstrated the most significant differences. Thus, we hypothesized that signatures of immature neutrophils and dysregulated granulopoiesis are present long-term in individuals reporting PASC, and that they correlate with PASC-related cognitive impairment. To test this hypothesis and its primary outcomes, we evaluated neutrophil phenotypes and granulopoiesis-related soluble factors between individuals reporting full recovery and those with PASC in two analytical timepoints (TP1, 6–18 months post-infection and TP2, 19–36 months post-infection). These timepoints were established as an operational analytical framework, rather than as biologically distinct stages of PASC. We observed signatures of immature neutrophils and dysregulated granulopoiesis in both time points and evaluated their associations with PASC development. Our findings provide exploratory insight into long-term PASC and potential immune-PASC associations, and may contribute to future improved understanding and management of PASC symptoms.

2 Materials and methods

2.1 Study design and cohort demographic characteristics

In this cross-sectional study, seventy-seven participants were recruited during 2021–2022 from the Faculty Hospital Brno in Czechia. Individuals were identified from the clinical records of the Faculty Hospital Brno and contacted via phone call. Participants were recruited irrespective of persistent symptoms and were subsequently classified as REC or PASC according to their recovery status at study enrolment. All participants had undergone PCR testing to confirm SARS-CoV-2 positivity at the time of infection, during 2020-2021. Data on the viral variant were not available for the recruited cohort; however, the disease was associated with the Wild-type, Alpha or Delta variants because of their high prevalence at that time (3). Classification of participants was done based on self-reported health status: 40 individuals reporting issues with COVID-19 recovery and 37 age-matched volunteers reporting full recovery from COVID-19 (REC). Subjects were enrolled at two time points (non-paired samples): from 6 up to 18 months (TP1) or from 19 up to 36 months (TP2) after COVID-19 onset. The 18-month cutoff was chosen given that at the time of study design, 18 months represented the longest known/established post-COVID period, while 36 months represented a deliberately longer-term follow-up. Specifically, we defined the 36-month time point as a longer-term follow-up period, corresponding to twice the then established interval. In order to validate that the groups are distinct and non-overlapping, the median, interquartile range (IQR), standard deviation, skewness, and kurtosis for each of the four groups (Supplementary Table 1) were extracted.

Both male and female participants were recruited for the study (Table 1). Three of the patients that were recruited in TP1, also were recruited in TP2 during a follow-up visit, otherwise each time point was comprised of different individuals. The 18-month cut-off was selected based on previous studies showing cognitive decline at up to 18 months after SARS-CoV-2 infection (27, 28) in order to distinguish participants in the established chronic phase of PASC (TP1), from those with a potentially even more long-term cognitive burden (TP2).

Inclusion criteria were: age 18–65 years with a history of SARS-CoV-2 infection, at least three months after the acute phase of the PCR-verified SARS-CoV-2 infection, complete recovery or persistent symptoms (REC and PASC groups respectively), a negative SARS-CoV-2 PCR test at the time of enrolment and native-level proficiency in Czech or Slovak, due to the requirements of the cognitive assessments. The race and education levels of the individuals were not considered as inclusion/exclusion criteria. Patient disease severity was assessed according to the WHO guidelines for the management of COVID-19 (WHO Reference Number: WHO/2019-nCoV/clinical/2021.2) and patients fulfilling the criteria of moderate-to-severe disease were included in the study, while critical cases (sepsis, septic shock, organ failure) were excluded. Four patients out of the cohort required oxygenation, with the rest of the patients not needing hospitalization. The four patients did not belong to a specific group of the study, but were spread among the groups PASC-TP1 and PASC-TP2. Further exclusion criteria were: pre-existing psychiatric disease or known cognitive deficits prior to COVID-19; organic brain disorders predating COVID-19; pregnancy; persistent SARS-CoV-2 PCR positivity; history of severe COVID-19 or post-intensive care syndrome; and evidence of trauma or pathological findings in brain imaging.

2.2 Assessment and scoring of cognition and quality of life

PASC or REC classification was based on self-reported incomplete or full recovery, based on direct questioning at the time of enrolment. Participant symptom presence and for at least one persistent symptom from the Newcastle post-COVID Syndrome

Follow-Up Screening Questionnaire (NC), at the time of enrolment, with total symptom count referred to as the NC score. Cognitive testing was performed by a trained psychologist with a battery of tests evaluating visuospatial functions, memory, attention and executive functions. The tests were including Rey–Osterrieth complex figure (29), Verbal fluency test - letters (30), Rey Auditory Verbal Learning Test (31), Brief Visuospatial Memory Test-Revised (32), Wechsler Adult Intelligence Scale – Memory for Digit Span (33), Trail making test (34), Neuropsychological & Visuospatial Assessment Battery – Mazes (35), and Cognitive Failures Questionnaire (36).

2.3 Blood sampling and processing

Blood samples were processed within 2 hours of collection. Whole blood (0.25 mL) was stabilized using Whole Blood Cell Stabilizer (cat. No. hWBCS002-100, Cytodelics AB, Sweden) at a 1:1 ratio and incubated at room temperature (RT) for 15 minutes. Plasma was obtained by centrifugation at 2,500 × g for 15 minutes at 4 °C. Stabilized blood and plasma samples were stored at −80 °C until use.

2.4 Flow cytometry profiling

Deep immunophenotyping was performed on stabilized whole blood samples from all 77 patients. Samples were thawed at 37 °C, diluted 1:5 in Fixation buffer (cat. No. hC002-1000-D01, Cytodelics AB), and incubated at RT for 10 minutes. Red blood cells were lysed using Lysis buffer (m/hC002-1000-L01, 1:4 dilution, Cytodelics AB) for up to 15 minutes at RT. Cells were washed in Wash buffer (m/hC002-1000-W01, Cytodelics AB), blocked with Fc receptor (FcR) blocking solution (cat. No. 130-059-901, Miltenyi, USA) in MACS buffer (PBS with 2% FBS and 2 mM EDTA) for 15 minutes, and stained for 30 minutes at 4 °C (Supplementary Table 2). Precision count beads (cat. No. 424902, BioLegend, San Diego, CA, USA) at 20µl per well were added right before acquisition. Data were acquired on a Cytek AuroraTM spectral cytometer (Cytek, Fremont, CA, USA).

2.5 ELISA

ELISA was used to quantify TNF-α, IL-10, sTNFR1, sTNFR2, TGF-β, CXCL8, CXCL12, IL-3, and G-CSF in plasma using DuoSet kits (R&D Systems, Minneapolis, MN, USA), following the manufacturer's instructions. Readouts were obtained with a Thermo Multiscan plate reader (Thermo Fisher Scientific, Waltham, MA, USA).

2.6 Flow cytometry data analysis

Data were analyzed using FlowJo® v10.10 (FlowJo LLC, Ashland, OR, USA). Cytometer setup and tracking (CST) beads (cat. No. 642412, BD Biosciences, USA) were used before each run to calibrate cytometer parameters. Total cell counts per ml of blood, for each sub-population during gating for neutrophils, were calculated based on the Precision count beads (cat. No. 424902, BioLegend, San Diego, CA, USA) manufacturer's protocol.

For the flow cytometry data, we compiled and optimized a new custom analysis pipeline, combining manual gating with high parameter clustering. Initially, quality control was performed on the samples, based on the built-in sample quality control of FlowJo, to make sure that the overall quality of the samples is adequate and that no fluorochromes were missing. Then, removal of outlier events/cleaning was performed with the algorithm PeacoQC, that removes events with fluorescences that are too different from the mean fluorescent values per sample (37). Briefly, the sensitivity of the isolation tree (IT) and the threshold for median absolute deviation (MAD) from the expected peak positions, controlling the strictness of the PeacoQC algorithm, were tuned. Tuning was done by running the algorithm on the common runs' samples with values 0.5-0.9 (IT) and 5-9 (MAD). The selected parameters were 0.8 and 8 respectively, in order to remove only strong outliers and keep as many intact events as possible for downstream analysis. Preliminary gating was performed in the raw data, in order to ensure that all populations were present and visualized properly. The raw and unmixed data were also overlapped to ensure proper unmixing and remove artifacts. To monitor batch effects, each plate included a common healthy donor sample (not included in the results). Batch effects were corrected using the CytoNorm algorithm (38) within FlowJo v10.10. The normalized samples were gated manually for the populations of interest and then subjected to principal component analysis (PCA) for outlier detection. The analysis was done based on the median fluorescence intensity (MFI) of all lineage markers for all cell populations per sample, after gating for each population. Outliers were detected and removed based on their place on the PCA plot and the 3x standard deviation (SD) method. The remaining samples were subjected to down-sampling (removal of a specific number of events in a randomized and unbiased way) to a total of 394397 neutrophils per condition, with the FlowJo plug-in Downsample v3, to ensure equal event number in every sample, equal representation of each individual in the consensus dataset, and to reduce potential bias, before downstream analysis. Dimensionality reduction was performed based on all lineage markers of all cell populations included in the panel, with the t-distributed stochastic neighbor embedding (t-SNE), employed to preserve local differences and preserve subgroups within each cell population. The t-SNE was performed within FlowJo v10.10, with a perplexity of 30, and 20 neighbors, after optimization. Because of the down-sampling prior to the dimensionality reduction and the clustering, any exported data on the clusters are presented as frequencies of total cell populations as a more representative parameter of cluster abundance, and not for the absolute cell counts per ml of blood.

Clustering of the neutrophil flow cytometry data was performed after normalization and dimensionality reduction, described above. The FlowSOM algorithm (39), based on self-organizing maps and unsupervised meta-clustering of those maps, was employed for the clustering, in order to preserve the structure of the data and the subpopulation differences, combined with the available computational power. Neutrophil lineage markers CD66b, CD16 and the functional markers CD62L, CD47, CD11b, CD336, CCR2, CD354, CX3CR1, CXCR2, CXCR4, HLA-DR were used for the clustering. Briefly, the number of meta-clusters was first set to 2 and

progressively increased until the creation of extra meta-clusters produced redundant marker patterns, in more than 1 populations. The optimal cluster number was decided as the highest number of meta-clusters, that didn't produce redundant marker patterns. In our data, the number of meta-clusters was decided as 10 meta-clusters after optimization. Statistical significance for the classification of cells into clusters was performed by the internal statistical tests of the algorithm. Additionally, the sub-populations of interest were gated for each participant, within the FlowSOM-produced clusters, in order to evaluate the frequencies of these sub-populations for each time point. The identity and frequency of these populations was also validated by completely manual and independent gating of the data, and overlapping the produced events, as well as the FlowSOM clusters, on the t-SNE plot.

2.7 Correlation and discriminant analyses

Correlations between all soluble factors and PMN-MDSC signature marker MFIs, were done using Spearman's pairwise non-parametric correlation with a significance p-value cutoff of 0.05. The non-parametric correlation was selected after assessing the normality of the data, described in detail below. The correlation analysis of the cytokine and chemokine data was performed in the R v4.4.3 environment.

The flow cytometry -derived marker MFIs and the ELISA -derived cytokine values were used for spatial partial least squares analysis (sPLSDA). The sPLSDA was initially tuned, to determine performance errors as the number or principal components used was increasing. The optimal number of principal components was set as 6, since the performance error was markedly reduced from this point on. The sPLSDA loadings on principal components 1 and 2 were extracted and used to determine the biggest contributors to each group and time point.

2.8 Clinical data analysis

Clinical analysis involved outlier detection, propensity matching and regression analysis. The demographic patient data used for propensity matching were age, sex and BMI. Only complete cases with all necessary demographic information were used in subsequent analyses. Because of the limited size of our cohort, we performed full matching to include as many patients as possible from all conditions (nREC-TP1 = 15, nREC-TP2 = 8, nPASC-TP1 = 5, nPASC-TP2 = 15 after matching), and we used a caliper of 1 to account for the slight mismatch in the age of the REC vs PASC groups in each time point. Standardized mean differences (SMDs) for TP1 for sex, age and BMI were -0.3333, 0.5634 and 0.996 for the original data and -0.0370, -0.0233 and 0.1765 for the matched data. For TP2 the SMDs were 0.7144, 0.4650 and 0.4527 for the original data and -0.1361, 0.0000 and 0.2935 for the matched data (Supplementary Table 3). All the propensity matched individuals (effective sample size per group: n=20 and n=23) were used for each of the GAMs for each time point. After matching, generalized additive models (GAMs) were used to evaluate associations between number of symptoms, cognition scores and immunological signatures. The data subjected to outlier detection were immunological signatures and soluble plasma factors, determined throughout the study. All curated data were used for regression analysis.

The GAMs were fitted separately for each time point, to account for non-linear relationships and correlations among variables. Non-linear effects were modeled using thin plate regression splines with penalized smoothing (gamma = 0.5) to control flexibility and overfitting. The basis dimension was set to k = 5 due to the limited sample size. For each time point and cognitive parameter, smooth-term p-values were adjusted using the Benjamini–Hochberg test (FDR = 0.05) to limit increasing exploratory sensitivity. Correction was applied when all smooth terms were significantly associated with the assessed cognitive parameter. Given the unequal group sizes and limited PASC-TP1 sample, a *post-hoc* sensitivity analysis (two-tailed, $\alpha = 0.05$, power = 80%) was performed separately at each time point. Model performance and potential overfitting were evaluated by assessing the explained variance, basis dimension checks (k-index), concurvity analysis, and effective degrees of freedom (EDF). All models showed adequate fit and no evidence of overfitting. All analyses were conducted in R (v4.4.3). Principal component analysis was performed using the FactoMineR package (v2.11) (40). Propensity score matching was done with the MatchIt (41) and optmatch (42) packages. Sparse partial least squares discriminant analysis (sPLSDA) was conducted with mixOmics (43), and correlograms were generated using corrplot (44).

2.9 Statistical analysis and sample size

Statistical analyses were performed using Prism® (GraphPad Software, La Jolla, CA, USA) and R (v4.4.0). Normality was assessed using the Shapiro-Wilk test. Comparisons between REC and PASC groups at each time point (REC-TP1 vs PASC-TP1 and REC-TP2 vs PASC-TP2) were made using non-parametric unpaired t-tests. Non-parametric effect sizes (Cliff's Delta) and 95% confidence intervals were assessed at TP1 and TP2. Comparisons at each time point and for each marker were performed independently, therefore, raw p-values are reported unless otherwise specified. For pairwise correlations and GAMs, p-values were adjusted for multiple comparisons using the Benjamini–Hochberg false discovery rate (FDR), with cutoffs of 0.1 (10%) and 0.05 (5%), respectively. Given the limited sample size, these analyses were considered exploratory. Any deviations from these tests are detailed in the corresponding figure legends or results sections. Data are presented as individual points with median values. Statistical significance was defined as follows: * (P <0.05), ** (P <0.01), *** (P <0.001) and **** (P<0.0001). A total of 77 patient samples were analyzed, for either time point independently with different patients participating in each time point (cross-sectional study).

3 Results

3.1 Self-reported PASC individuals show cognitive defects and worsened clinical status up to 3 years post-COVID-19

In the first stage of the analysis, we assessed the clinical status and cognitive state of our cohort and determined whether self-reported PASC is followed by poorer cognitive test scoring.

Following cognitive evaluation, patients with complete clinical data were included for downstream experimental procedures (Figures 1A, B), while those with missing data were excluded. Participants were classified according to the time of blood sampling for immunological evaluation as TP1 (6–18 months post-COVID-19) or TP2 (19–36 months). The 18-month cut-off was based on previous studies reporting immune alterations, antibody persistence, and cognitive symptoms at 12–18 months after SARS-CoV-2 infection (27, 28), while follow-up beyond 24 months remains less studied. Thus, comparing independent REC and PASC cohorts at TP1 and TP2 allowed assessment of immune and cognitive alterations across distinct intervals since infection. Since the 18-month cutoff was chosen conceptually, we first validated that our groups for each time point are distinct and non-overlapping by extracting the median, interquartile range (IQR), standard deviation, skewness, and kurtosis for each of the four groups (Supplementary Table 1). According to our descriptive statistics' data, the sampling times for all groups showed concentrated distributions around their

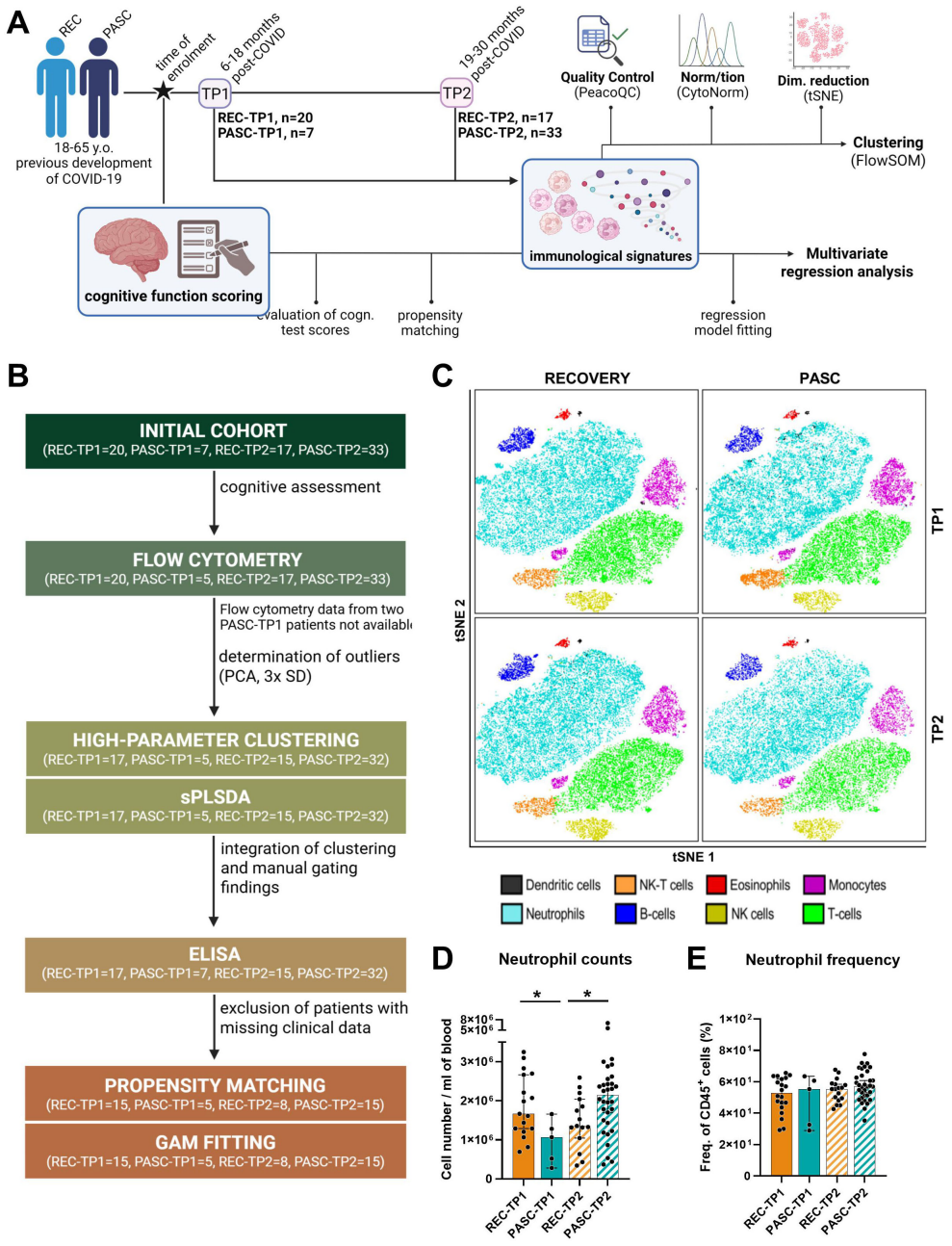


FIGURE 1
Increased mature and reduced immature neutrophils in PASC individuals are sustained at 18 months post-COVID-19. **(A)** Workflow illustrating patient sample collection and phenotyping of immune cells and plasma soluble factors. **(B)** Flowchart depicting all the individuals initially assessed, exclusions, numbers per group and per timepoint, and the analyses type. **(C)** t-stochastic neighbor embedding (tSNE) plot showing clustering of major immune cell populations based on differentially expressed lineage markers. Dimensionality reduction was performed with the Barnes-Hut algorithm (perplexity = 30, 1000 iterations) in FlowJo v.10.10. **(D)** Total counts per ml of blood of neutrophils, defined as $CD45^+CD3^-CD19^-CD56^-CD66b^+$ granulocytes. **(E)** Neutrophil frequency as a percentage of total leukocytes ($CD45^+$ cells). Data are presented as median with 95% confidence interval (CI). $n_{REC\text{-}TP1} = 17$, $n_{REC\text{-}TP2} = 15$, $n_{PASC\text{-}TP1} = 5$, $n_{PASC\text{-}TP2} = 32$, $^* P < 0.05$.

respective medians, together with variability and asymmetric tails. This suggested that our groups are distinct and non-overlapping, but also pointed to the presence of "extreme" non-outlier values, close to the 18-month cutoff, or towards the upper of lower end of the time periods (towards 6 or 36 months respectively). We then visualized the exact distribution of the sampling times for REC and PASC groups, for both time points together (Supplementary Figure S1A). We saw that our cohort showed a distinct gap around the 18-month cutoff and concentration around ~14 months for TP1 groups, and around ~26 months for the TP2 groups. These results suggested that the 18-month cutoff reasonable in the context of our study, although it doesn't represent a biologically or clinically discrete boundary between two fundamentally different post-COVID-19 phases. Based on our cohort and time point separation, we evaluated the Newcastle post-COVD-19 Syndrome Follow Up Screening questionnaire scores (NC score) to estimate the overall impairment (number of symptoms), and the following neuropsychological assessments of memory, attention and executive function: Rey–Osterrieth complex figure (Rey_copy, Rey_ov1, Rey_ov2), Verbal fluency test - letters (VF_total), Rey Auditory Verbal Learning Test (learning and immediate recall after the last trial as AVLT_5, overall performance in the immediate recall as AVLT_T, delayed recall after inference as AVLT_6, delayed recall after 30 minutes as AVLT_OV), Brief Visuospatial Memory Test-Revised (recognition as BVMT_R, delayed recall as BVMT_OV, overall performance as BVMT_T), Wechsler Adult Intelligence Scale – Memory for Digit Span (OC), Trail making test (TMT_A, TMT_B), Neuropsychological Assessment Battery – Mazes (Mazes_total) (Table 2). The NC scores and cognitive tests were completed and assesses at the time of participant enrolment. We observed increased NC_scores in PASC patients in both the TP1 and the TP2 cohorts (Table 2). We also observed a significant decrease in Rey–Osterrieth complex figure -related tests in TP1. AVLT immediate recall scores remained unchanged, however delayed-recalls (after inference and 30 minutes later) scores were significantly decreased in PASC at TP1 compared to REC. Digit span test scores were similar between groups, but OC_B backward scores were significantly lower in PASC-TP2 compared to REC-TP2, suggesting impairments in attention or working memory in the participants of this time point. TMT-B completion times were prolonged in PASC at both time points, reflecting poorer performance and reduced cognitive flexibility. Finally, the cognitive failure scores were higher in PASC participants in TP2 indicating more self-reported frequent cognitive deficits overall.

Together, these findings confirm the self-reported categorization of the participants as REC or PASC by indicating an overall higher cognitive symptom burden in PASC individuals. Interestingly, the PASC burden is also evident in individuals enrolled from 19 months, up to 36 months post-infection, thus extending the known timeframe where PASC cognitive decline is reported until now. Verbal and visuospatial memory impairments were evident at the TP1 individuals, which can be related to deficits in episodic memory processes, executive functions or attention in this time point. Differences in cognitive performance were also evident in TP2 individuals. However, due to the deficits not being apparent at every subtest, but only at several of them, we can attribute the differences to deficits in retrieval of information from memory, or in maintenance of attention. It is important to note that the potential presence of ambulatory patients, or the fact that some of the individuals refused to participate, might pose a limitation to these findings. However, overall, these patterns point to broad cognitive involvement rather than isolated deficits, in PASC individuals.

3.2 A shift from immature to activated neutrophils reflects immune remodeling in PASC individuals at 18 months post-COVID-19

In order to understand how long-term immune remodelling might contribute to PASC, we first compared immune cell phenotypes between REC and PASC individuals at each of the two time points independently. To do so, we performed flow cytometry and ELISA to analyze immune cell phenotypes (Figure 1A). Because of the cross-sectional nature of the study, and the fact that mostly different individuals were recruited and measured per time point, we focused on the differences between REC and PASC at the time of measurements (REC vs PASC for either the TP1 cohort, or for the TP2 cohort) and not the longitudinal differences between the TP1 and TP2 cohorts. The whole initial study number of individuals was subjected to flow cytometry measurement, with the exception of two REC-TP1 individuals for which the data was not acquired (Figure 1B). The measured data was subjected to outlier detection via principal comment analysis (PCA) and then processed for ELISA and clinical analysis (Figure 1B). Dimensionality reduction using the t-stochastic neighbor embedding (t-SNE) algorithm, was applied to all identified immune cell populations, including neutrophils ($CD16^+CD66b^+$), eosinophils ($CD193^+$), monocytes ($CD14^+$), NK cells ($CD3^-CD56^+$), NK-T -like ($CD3^+CD56^+$) cells, T-cells ($CD3^+CD19^-$) and B-cells ($CD19^+$) (Figure 1C, Supplementary Figure S1B). All the aforementioned lineage markers were used for the construction of the t-SNE (Supplementary Figure S1B). In doing so, we observed marked differences in the distribution of neutrophils in PASC versus REC across both time points. This was evidenced by altered pattern of events in the cluster of neutrophils on the t-SNE plot, with several areas in PASC-TP1 being less dense in comparison to REC-TP1 (Figure 1C). This finding suggested reduction of several sub-populations of neutrophils to a much bigger extent than in other cell populations. To elaborate on this finding and determine quantitative changes in neutrophil counts or frequency, we gated for neutrophils, defined as $CD45^+CD3^-CD19^-CD56^-CD66b^+$ granulocytes (Supplementary Figure S1C). We observed changes in several of the parent populations of neutrophils. Namely we saw a significant decrease in cell number of $CD45^+$ leukocytes per ml of blood, in the PASC-TP1 compared to REC-TP1, and an increase in PASC-TP2 compared to REC-TP2 (Supplementary Figure S1D). We saw a similar pattern in $CD3^-CD19^-$ myeloid cells (Supplementary Figure S1E) but only trends in $CD3^+CD19^-$ lymphocytes (Supplementary Figure S1E). Additionally, we found a similar pattern in granulocytes but only a trend in non-granulocytes (Supplementary Figure S1F), and no significant changes in $CD66b^+CD56^-$ cells (Supplementary Figure

10.3389/fimmu.2026.1885356

TABLE 2 Newcastle and cognitive scoring for REC and PASC individuals throughout the study.

TP	Parameter	REC median (IQR)	PASC median (IQR)	P (two-sided)	Cliff's delta	95% CI low	95% CI high	Sign.
TP1	NC_score	2 (0–4)	8 (8–10)	0,000	-0,978	-1,000	-0,867	***
TP1	Rey_copy	36 (36–36)	35 (35–35)	0,019	0,575	0,113	0,950	*
TP1	Rey_ov1	28.5 (24–29.2)	21 (20–21)	0,026	0,663	0,263	0,938	*
TP1	Rey_ov2	28.5 (22.8–29.2)	20 (19–20)	0,030	0,638	0,225	0,925	*
TP1	VF_total	43.5 (35.8–54.5)	37 (35–48)	0,505	0,213	-0,350	0,725	
TP1	OC_F	9.5 (8.8–11.2)	9 (8–9)	0,480	0,225	-0,350	0,738	
TP1	OC_B	8 (6–8.2)	5 (5–9)	0,447	0,238	-0,438	0,888	
TP1	OC_total	17 (16–19.2)	14 (13–17)	0,316	0,313	-0,325	0,875	
TP1	AVLT_5	12.5 (12–14)	12 (11–14)	0,476	0,225	-0,400	0,813	
TP1	AVLT_6	12.5 (11–13.2)	9 (8–11)	0,043	0,613	0,100	0,975	*
TP1	AVLT_OV	12 (11–13)	10 (8–12)	0,204	0,388	-0,238	0,925	
TP1	AVLT_T	53.5 (50.8–57.5)	47 (46–54)	0,159	0,438	-0,113	0,875	
TP1	BVMT_OV	11.5 (11–12)	12 (12–12)	0,424	-0,238	-0,688	0,325	
TP1	BVMT_R	12 (12–12)	11 (11–12)	0,063	0,475	0,013	0,938	
TP1	BVMT_T	31.5 (28–35)	29 (28–30)	0,299	0,325	-0,150	0,738	
TP1	TMT_A	29 (22.8–34)	39 (30–40)	0,214	-0,388	-0,825	0,100	
TP1	TMT_B	52.5 (45.8–64.2)	80 (77–95)	0,010	-0,750	-1,000	-0,375	*
TP1	Mazes_total	23 (19.5–25)	22 (19–24)	0,673	0,138	-0,475	0,713	
TP1	CFQ	30.5 (21.5–40.2)	53 (31–68)	0,048	-0,600	-1,000	-0,100	*
TP2	NC_score	0 (0–3)	6 (5–7.8)	0,000	-0,769	-0,967	-0,513	***
TP2	Rey_copy	36 (36–36)	36 (34–36)	0,056	0,364	0,065	0,628	
TP2	Rey_ov1	26 (22.5–28.5)	21 (16–28)	0,225	0,268	-0,121	0,628	
TP2	Rey_ov2	24 (21–28)	23 (17–28)	0,658	0,100	-0,320	0,498	
TP2	VF_total	38 (35–45)	41 (29–42)	0,486	0,156	-0,268	0,541	
TP2	OC_F	10 (9–10.5)	8 (7–9)	0,039	0,446	0,065	0,788	*
TP2	OC_B	8 (8–9)	6 (4–7)	0,002	0,632	0,307	0,896	**
TP2	OC_total	18 (16.5–19.5)	14 (13–16)	0,003	0,632	0,316	0,887	**
TP2	AVLT_5	13 (12–14)	12 (11–14)	0,511	0,143	-0,242	0,519	
TP2	AVLT_6	12 (9.5–12.5)	10 (9–13)	0,481	0,156	-0,255	0,563	
TP2	AVLT_OV	12 (9.5–13)	10 (9–12)	0,359	0,203	-0,216	0,610	
TP2	AVLT_T	54 (49.5–55)	51 (44–56)	0,628	0,108	-0,303	0,519	
TP2	BVMT_OV	12 (10–12)	11 (10–12)	0,493	0,147	-0,260	0,528	
TP2	BVMT_R	12 (12–12)	12 (12–12)	0,591	-0,087	-0,364	0,147	
TP2	BVMT_T	31 (29–33.5)	30 (26–32)	0,247	0,255	-0,177	0,641	
TP2	TMT_A	25 (20–29.5)	34 (25–38)	0,034	-0,459	-0,779	-0,078	*
TP2	TMT_B	55 (43.5–58.5)	76 (65–88)	0,000	-0,758	-1,000	-0,394	***
TP2	Mazes_total	21 (20–25)	19 (12–25)	0,174	0,299	-0,087	0,649	
TP2	CFQ	27 (21–33)	34 (27–45)	0,098	-0,364	-0,701	0,017	

Data for each cognitive parameter are presented as median (+/- interquartile range; IQR). Statistical significance between REC and PASC for each time point is marked as *P<0.05, **P<0.01, ***P<0.001. NC_score; Newcastle post-COVID Syndrome Follow-Up Screening Questionnaire score, Rey_copy; Rey–Osterrieth complex figure, Rey_ov1; Rey–Osterrieth complex figure Immediate Recall, Rey_ov2; Rey–Osterrieth complex figure Delayed Recall, VF_total; Verbal fluency test, letters total score, OC_F; Wechsler Adult Intelligence Scale, Memory for Digit Span Forward score, OC_B; Wechsler Adult Intelligence Scale, Memory for Digit Span Backwards score, OC_total; Wechsler Adult Intelligence Scale, Memory for Digit Span total score, AVLT5; Rey Auditory Verbal Learning Test - learning and immediate recall after the last trial, AVLT6; Rey Auditory Verbal Learning Test - delayed recall after inference, AVLT_OV; Rey Auditory Verbal Learning Test - delayed recall after 30 minutes, AVLT_T; Rey Auditory Verbal Learning Test - overall performance in the immediate recall, BVMT_OV; Brief Visuospatial Memory Test-Revised - delayed recall, BVMT_R; Brief Visuospatial Memory Test-Revised, recognition, BVMT_T; Brief Visuospatial Memory Test-Revised - overall performance, TMT_A; Trail making test part A, TMT_B; Trail making test part B, Mazes_total; Neuropsychological Assessment Battery, Mazes, CFQ; Cognitive Failures Questionnaire.

S1G). Most importantly, we found the same pattern in neutrophils, meaning a decrease in neutrophil number per ml of blood (Figure 1D) in the PASC-TP1 compared to REC-TP1, and an increase in PASC-TP2 compared to REC-TP2, suggesting that neutrophil -related alterations are evident both in TP1 (from 6 up to 18 months) and in TP2 (from 19 up to 36 months post-COVID). Interestingly, however, the overall frequency of neutrophils among $CD45^+$ cells did not differ between groups (Figure 1E), suggesting perhaps that the observed changes might have also occurred at the subset level. Overall, these findings show significant changes in neutrophil/granulocyte -related lineage, both in the TP1 and in the TP2 cohorts. Additionally, while lymphoid cell/adaptive immunity alterations have been documented in PASC (45, 46), insight into myeloid cells remains elusive. Based on the above, we focused any following analysis on neutrophils to better characterize the observed changes in PASC.

3.3 Reduced immature neutrophils indicate/support altered granulopoiesis in PASC at 18 and 36 months post-COVID-19

In the next step of our study, we assessed neutrophil maturation and activation status by gating for CD16 and/or CD62L expression, or alternatively for CD66b and/or CD16 expression (Supplementary Figure S2A), as previously described (47–49). We also determined $CD16^+CD62L^{low}$ (activated/mature), $CD16^{low}CD62L^+$ (banded neutrophils), $CD16^+CD62L^+$ (mature segmented neutrophils) and $CD16^-CD62L^-$ (immature) neutrophils (Figure 1C) described before in respiratory infection or inflammation (50–52). Analysis of these maturation markers in both the TP1 and TP2 cohorts, revealed a higher frequency of $CD16^+CD62L^{low}$ (activated/mature) neutrophils in PASC compared to REC individuals, along with a corresponding decrease in $CD16^-CD62L^-$ (immature) neutrophils in TP1 (Figure 2A). Even though this shift toward a mature neutrophil phenotype was observed only at the TP1 cohort (6–18 months post-COVID-19), it suggests either persistent activation stimuli that promote maturation, or intrinsic changes in the phenotype of newly produced neutrophils. In parallel, the number of $CD16^-CD62L^-$ (immature) neutrophils per ml of blood was increased in the TP2 cohort in PASC-TP2 compared to REC-TP2 (Supplementary Figure S2B) without any significant difference in the rest of the subsets (Figures 2B, C). By contrast, the overall frequency of activated neutrophils ($CD16^+CD66b^+$) did not significantly differ between REC and PASC groups in neither TP1 nor TP2 individuals (Supplementary Figure S1D), whether assessing activated and degranulating neutrophils ($CD16^+CD66b^+$) or less activated subsets ($CD16^+CD66b^{low}$). However, we observed several trends in the number of these subsets, per ml of blood (Supplementary Figure S1E), specifically, a trend to decrease both $CD16^+CD66b^+$ and $CD16^+CD66b^{low}$ neutrophils in PASC-TP1 compared to REC-TP1 and a trend or increase in PASC-TP2 compared to REC-TP2 (Supplementary Figure S1E). Together, these results indicate a shift in PASC individuals toward a more mature and activated neutrophil phenotype, characterized by reduced frequencies of immature subsets in TP1 individuals, and an increase of these subsets in the cohort of TP2. Additionally, these results might reflect long-term alterations in neutrophil production or maturation, rather than transient activation responses. Nevertheless, the limited number of PASC-TP1 samples represents an important limitation and increases uncertainty around these observations.

Neutrophil maturation status affects their functional characteristics, including activation, cytokine production, and degranulation (48–50). By contrast, immature neutrophils—particularly PMN-MDSCs—exhibit immunosuppressive properties (21, 53). Given the above results on neutrophil subsets observed in PASC individuals in TP1 or TP2, we next sought to characterize neutrophil functional heterogeneity and identify distinct subpopulations that might contribute to PASC. To do so, we applied the Flow SOM algorithm to cluster neutrophils from all participants at both time points, using lineage (CD16, CD66b, CD62L) and functional (CD11b, CD47, CD336, CCR2, CX3CR1, CXCR2, CXCR4, HLA-DR) markers. We identified six functionally distinct neutrophil clusters, each displaying either time point–specific or persistent group-related changes in cluster size. The distribution of cells in separate clusters was based on the internal statistics of the flowSOM algorithm. These differences in cluster abundance were most pronounced in the TP1 cohort, between REC and PASC, but were also evident in TP2 individuals (Figure 2B). This finding, coupled with our previous findings on total number alterations of neutrophils and neutrophil subsets in both time points, suggests dynamic functional shifts of the neutrophil population in PASC that can be present at least up to 18 months post-infection.

Clusters 1, 3 and 4 were characterized as $CD16^{+/bright}CD62L^+$, consistent with a not yet fully activated neutrophil state. Cluster 2 was characterized as $CD16^+CD62L^{low}$ consistent with an activated state of mature neutrophils (54). Finally, clusters 5 and 6 were characterized as $CD16^{+/dim}CD62L^{dim/-}$, consistent with immature or suppressive neutrophils (47, 55). Each of the six clusters exhibited a unique marker signature and showed varying degrees of similarity with one another (Supplementary Figure S3A). Clusters 1 and 3 were most closely related, as were clusters 2 and 4. Clusters 5 and 6 were distinct from the others but closely associated with each other, sharing similar activation marker profiles despite some differences across conditions. On the t-SNE plot, clusters 5 and 6 were spatially separated from the rest of the neutrophil population (Figure 2B), suggesting a unique lineage or functional role. Cluster 5 was markedly reduced in PASC compared to REC in the TP1 cohort (Figure 2C, upper plot), while in the TP2 cohort there was no significant difference between PASC and REC. On the contrary, cluster 6 was largely depleted in PASC-TP2 compared to REC-TP2 (Figure 2C, lower plot).

In order to characterize these clusters based on specific markers in the cohorts recruited in each time point, we performed spatial partial least squares discriminant analysis (sPLSDA), using the mean fluorescence intensities (MFIs) of all measured markers (Figures 2D, E). We extracted the loadings of each marker on component 1, which captures the largest part of the discriminatory information between the identified clusters. The markers with the highest absolute loading values on component 1, had the strongest discriminatory contribution to the respective cluster, and therefore contributed the most to the separation. Since sPLSDA identified

10.3389/fimmu.2026.1885356

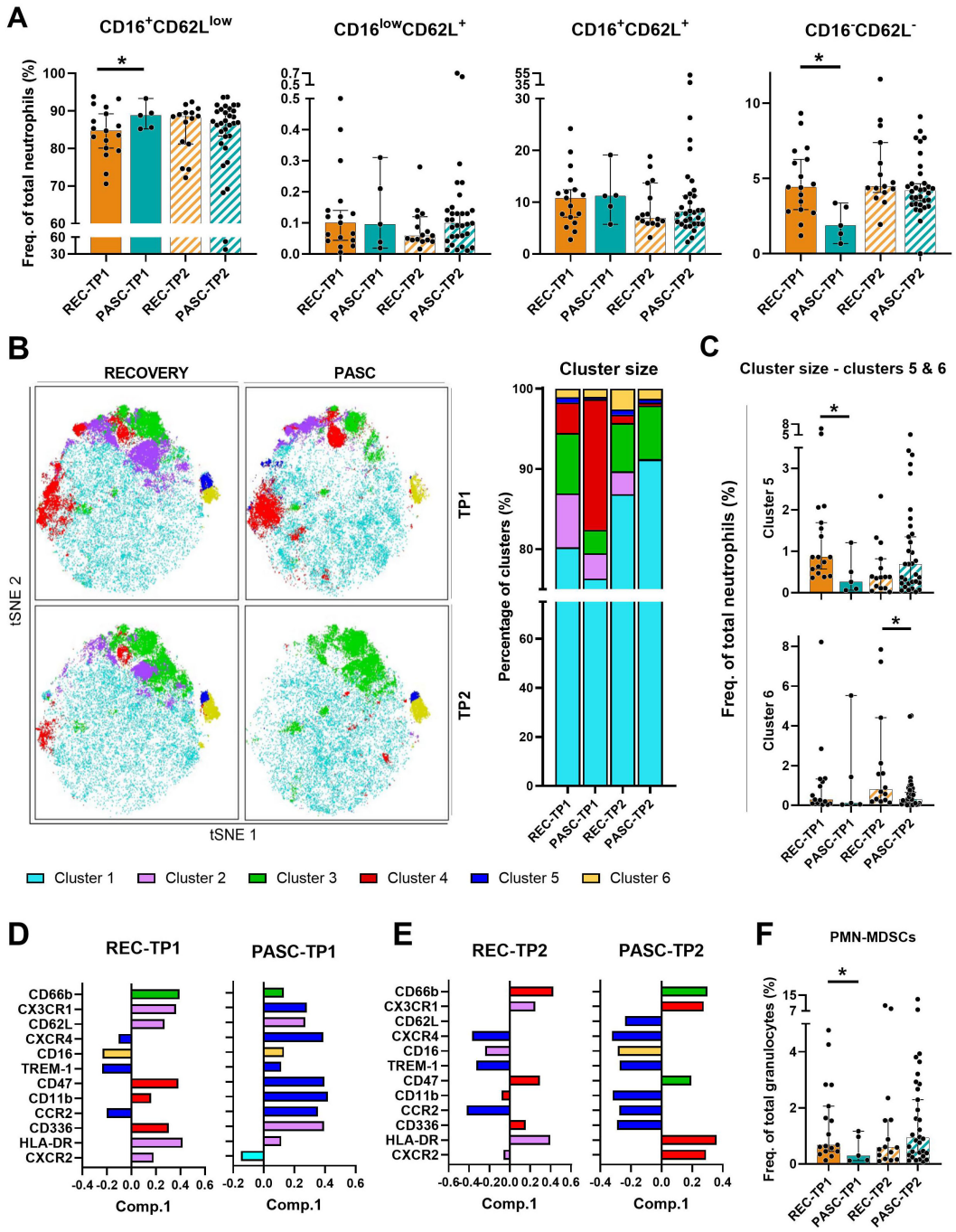


FIGURE 2
Reduced immature PMN-MDSC -like neutrophils support immune remodeling in PASC at 18 and 36 months post-COVID-19. **(A)** Frequencies of neutrophil subsets based on the expression of CD16 and CD62L, presented as % of total neutrophils. **(B)** tSNE plots showing distribution of neutrophil clusters by condition and time point (left) and barplot (right) with the median cluster size, as % of total neutrophils. Dimensionality reduction was done with the t-stochastic neighbor embedding (tSNE) algorithm, and was performed with the Barnes-Hut algorithm (perplexity = 30, 1000 iterations) in FlowJo v.10.10. **(C)** Cluster sizes (%) for clusters 5 and 6 across conditions for each of the cohorts and time points. **(D, E)** Sparse partial least squares discriminant analysis (sPLSDA) of median fluorescence intensities (MFIs) for functional markers used in clustering, for TP1 **(D)** and TP2 **(E)**, identifying marker signatures of each cluster. **(F)** Frequency of the manually gated PMN-MDSCs in each group. Statistical significance was assessed using the built-in test of the FlowSOM algorithm and internal statistical tests of the sPLSDA algorithm. Data are presented as median with 95% confidence interval (CI). $n_{REC\text{-}TP1}$ = 17, $n_{REC\text{-}TP2}$ = 15, $n_{PASC\text{-}TP1}$ = 5, $n_{PASC\text{-}TP2}$ = 32 patients. *$P < 0.05$.

variables (markers) that best discriminated each cluster from the rest simultaneously, the loadings are presented for the global model rather than for individual clusters (Figures 2D, E). In this way, we aimed to reflect the overall contribution of each marker to the separation of each cluster from the rest. Notably, cluster 5 was the cluster with the most distinct surface marker pattern for PASC individuals both in the cohort measured in TP1 and the one in TP2. This finding implies stable remodeling of the immature neutrophil compartment that is evident both up to 18 months and at up to 36 months post-infection. Although relative abundance can influence

sPLSDA, the prominence of cluster 5 in each of the time points, suggests an interdependent relationship between neutrophil dysregulation and PASC, possibly contributing to systemic alterations or cognitive symptoms. Cluster 5 was defined by CXCR4, TREM-1, and CCR2 expression across both REC and PASC groups, in the TP1 and the TP2 cohorts, while CD16 defined cluster 6 (Figures 2D, E). In TP1, cluster 5 showed increased expression of its signature markers (CXCR4, TREM-1, CCR2), along with CD11b, CX3CR1, and CD47, in PASC compared to REC. In TP2, cluster 5 was characterized by reduced CXCR4, TREM-1, and CCR2, with increased CD11b, CD336, and CD62L (Figure 2E). Importantly, CXCR4 and CCR2 (cluster 5) and CD16 (cluster 6) are expressed at distinct stages of neutrophil maturation (56, 57).

Given the phenotypes associated with clusters 5 and 6, we then aimed to determine their relationship with PMN-MDSCs, a subset of immature neutrophils with immunoregulatory properties known to drive immunosuppression (21, 25, 53, 58, 59). We identified PMN-MDSCs (defined as HLA-DR^{low}CD11b^{+}CD14^{-}CD66b$^{dim/+}$ cells) in all groups (60) (Supplementary Figure S3B). Interestingly, we observed for the first time a reduction in PMN-MDSCs in PASC versus REC of TP1, but no statistical difference between the REC and PASC individuals of TP2 (Figure 2F). This delayed depletion at TP1 and the lack of difference between REC and PASC PMN-MDSCs, in the TP2 individuals, indicated granulopoietic remodeling in both the TP1 cohort and the TP2 cohorts. Supporting this view, PMN-MDSCs overlapped spatially with clusters 5 and 6 on the t-SNE plot (Figure S3C), reinforcing the impaired neutrophil maturation in the TP1 cohort, but not in the TP2 cohort. Despite the limited sample size in REC-TP1, the concordance between manual gating and unsupervised FlowSOM clustering provided converging evidence supporting that the observed findings are biologically plausible. However, they should be considered exploratory and hypothesis generating, and need to be validated in larger cohorts.

3.4 Granulopoiesis and immunosuppression markers align with neutrophil remodeling in PASC

Thus far we have shown a reduction in PMN-MDSCs in PASC individuals, potentially reflecting dysregulated neutrophil maturation. To further explore the potential drivers of altered neutrophil maturation in PASC, we examined whether plasma levels of cytokines and other soluble factors were associated with PASC status. We evaluated the whole number of individuals that were subjected to cognitive assessment, including the two individuals without available flow cytometry data. ELISA revealed significant differences in plasma levels of the soluble TNF receptors sTNFR1 (TNFRSF1A) and sTNFR2 (TNFRSF1B) between REC and PASC individuals. Specifically, sTNFR1 was elevated, and sTNFR2 was reduced in PASC in the TP1 cohort (Figures 3A, B). Given that CXCR4 and CCR2 are signature markers of cluster 5, we also assessed plasma levels of their respective ligands, CXCL12 and CCL2. While CCL2 levels remained unchanged in PASC (Figure 3C), CXCL12 was significantly decreased in PASC compared to REC at TP1 (Figure 3D). In the TP2 cohort, we observed a modest but significant increase in both IL-3 and IL-6 levels in PASC compared to REC (Figures 3E, F). Meanwhile, levels of stem cell factor (SCF) showed a trend toward change across groups but did not reach statistical significance (Figure 3G).

Next, we hypothesized that the determined soluble molecules/receptors might correlate with the surface levels of PMN-MDSCs surface markers. To explore potential relationships between CXCL12, IL-3, IL-6 and soluble TNF receptors, and PMN-MDSC surface receptor CCR2, CXCR4 and TREM-1 expression, we conducted exploratory non-parametric Spearman's correlation analyses (Figures 3H, I). Variables included all measured soluble factors, the frequency of PMN-MDSCs, and the MFIs of their key surface markers. We implemented a significance threshold of 0.05 and controlled for type I errors for multiple comparisons using the Benjamini-Hochberg false discovery rate (FDR) test with a cutoff of 0.1 (10%) in order to explore as many potential correlations as possible. In the TP1 cohort, significant correlations were found among the three signature surface markers, between IL-3 and CXCL12 (corrected p-value = 0.014) and between the triad comprised of TREM-1, CCR2 and CXCR4 (corrected p-values for TREM-1-CCR2 = 0.003133339, CCR2-CXCR4 = 2.365541e-10, CXCR4-TREM-1 = 0.001161903) (Figure 3H). In the TP2 cohort, significant correlations again emerged between the signature surface markers and several cytokines, including CXCR4 with both CCR2 (corrected p-value = 4.158136e-06) and TREM-1 (corrected p-value = 0.01048935) and SDF with IL-13 (corrected p-value = 0.009673144) (Figure 3I). These findings suggest interconnections between plasma soluble factors and key PMN-MDSCs surface markers. Importantly, that expression of CXCR4 and CCR2 on PMN-MDSCs correlated with plasma IL-3 levels, even in the TP2 cohort. This association points to a possible link between altered granulopoiesis and PMN-MDSC dynamics in PASC, which warrants further investigation.

3.5 Cognitive decline in PASC is associated with granulopoiesis and neutrophil maturation signatures

In the final part of our study, we investigated whether the identified immunological signatures associate with cognitive dysfunction in PASC. Specifically, we explored correlations between immune dysregulation, neuroinflammation, and number of persistent symptoms (NC score) and cognitive performance (Figure 4) with multivariate modeling. We hypothesized that specific sets of PMN-MDSCs markers/soluble molecules might associate with higher or lower cognitive score in a linear or non-linear way. To assess whether immune alternations identified earlier were associated with overall symptom load (NC score) and cognitive impairment (Figures 4A-D), we first performed propensity matching between PASC and REC groups, controlling for age, sex, and BMI (Supplementary Table 3). Because of the limited size of our cohort, we performed full matching to include as many patients as possible from all conditions, and we used a caliper of 1 to account for the slight mismatch in the age of the REC vs PASC groups in the cohort of each time point. For the matching and the downstream analysis, we used all patients from each cohort, for who all cognitive and

10.3389/fimmu.2026.1885356

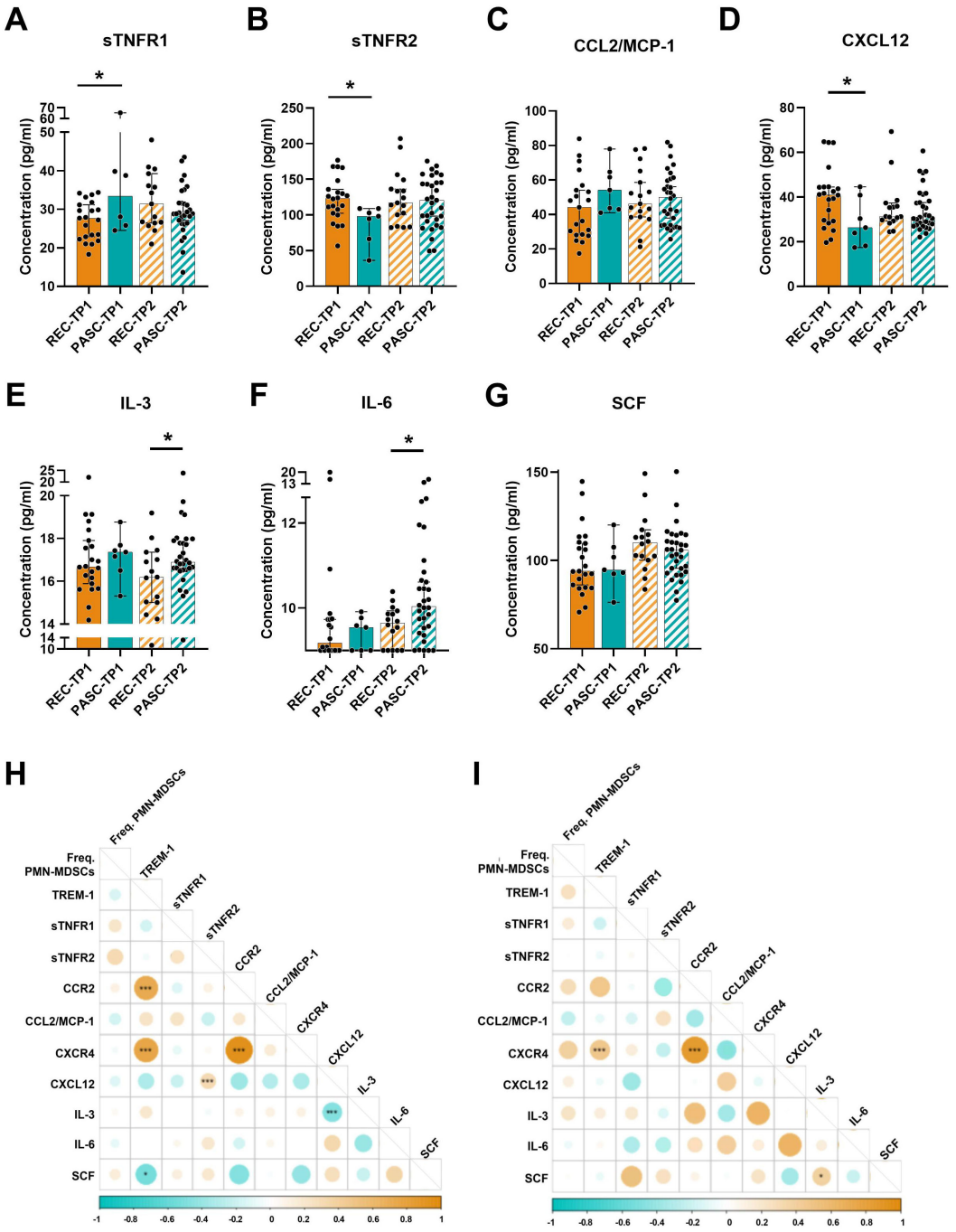


FIGURE 3
Granulopoiesis -related soluble factors characterize PASC-reporting individuals recruited at up to 18 or 36 months after COVID-19. **(A-G)** Plasma levels of soluble factors: **(A, B)** TNF receptors 1 and 2 (sTNFR1, sTNFR2), **(C)** monocyte chemotactic protein 1/chemokine ligand 2 (MCP1/CCL2), **(D)** CXC chemokine ligand 12 (CXCL12), **(E)** interleukin 3 (IL-3), **(F)** stem cell factor (SCF), **(G)** interleukin 6 (IL-6). **(H, I)** Correlograms showing pairwise Spearman correlations between all soluble factors and PMN-MDSC signature marker MFIs for **(H)** TP1 and **(I)** TP2. All analyses were performed in the R v4.4.3 environment. sPLSDA and correlation analysis included only complete cases with detectable levels of all measured cytokines. In the correlograms, orange indicates positive correlations and turquoise indicates negative correlations; color intensity and circle size are proportional to Spearman correlation coefficients. Data are presented as median with 95% confidence interval (CI). $n_{REC\text{-}TP1} = 17$, $n_{REC\text{-}TP2} = 15$, $n_{PASC\text{-}TP1} = 7$, $n_{PASC\text{-}TP2} = 32$. *$P < 0.05$, ***$P < 0.001$.

immunological information was available, independent of poorer or better scoring throughout the cognitive tests. Patients that remained unmatched were excluded from the following steps.

We then applied weighted generalized additive models (GAMs) and multivariate regression to evaluate associations between cognitive scores and either the previously identified PMN-MDSC surface markers (TREM-1, CXCR4, CCR2) or soluble immune factors (sTNFR1, sTNFR2, CCL2, IL-3, CXCL12, IL-6, SCF) for either the TP1 cohort, or the TP2 cohort. All the propensity matched individuals (effective sample size per group: n=20 and n=23) were used for each of the GAMs for each time point. Sensitivity analysis of the GAMs indicated that the study was

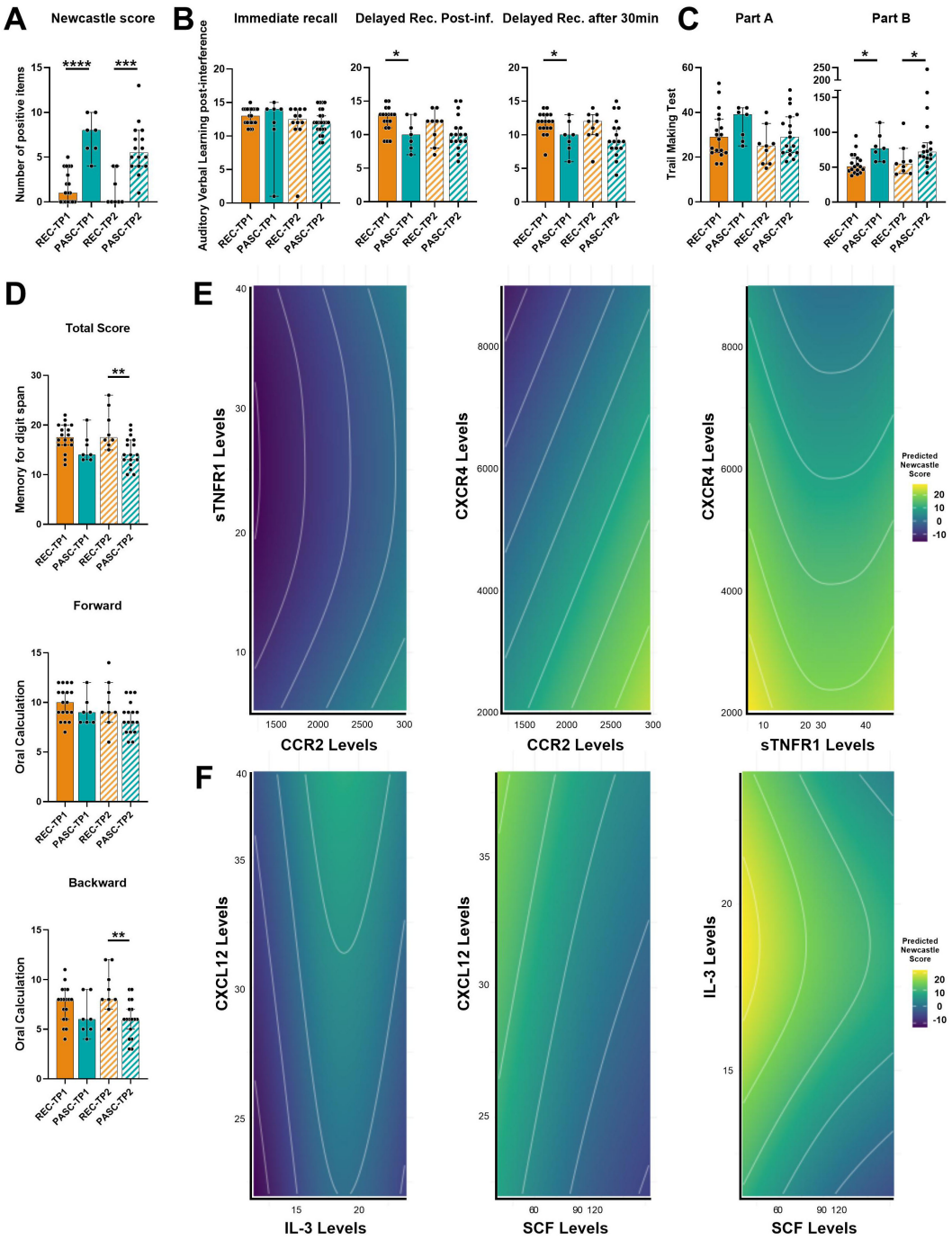


FIGURE 4
Immature neutrophil and granulopoiesis signatures are associated with cognitive dysfunction parameters in PASC-reporting individuals. **(A)** Newcastle (NC) score assessing clinical status **(B)** Auditory Verbal Learning Test (AVLT) scores for immediate (AVLT_5) and delayed recall post-inference (AVLT_6) or after 30 minutes (AVLT_OV), evaluating episodic memory **(C)** Trail Making Test (TMT) Part A and Part B scores, assessing attention, psychomotor speed, mental flexibility **(D)** Total, forward, and backwards digit span test (OC) scores for each time point. **(E, F)** Grid plots showing predicted NC scores based on paired combinations of immune factors from each immunological signature at **(E)** TP1 and **(F)** TP2. Plot colors indicate higher or lower predicted NC score. All analyses were performed on propensity-matched individuals across groups, controlling for age, sex and BMI. Data are presented as median with 95% confidence interval (CI). $n_{REC\text{-}TP1}$ = 15, $n_{REC\text{-}TP2}$ = 8, $n_{PASC\text{-}TP1}$ = 5, $n_{PASC\text{-}TP2}$ = 15 patients, *$P < 0.05$, ****$P < 0.0001$.

powered to detect large effect sizes of Cohen's d ≥ 1.427 and d ≥ 1.286 for TP1 and TP2 respectively. Thus, the results of the model fitting and multivariate analyses were considered exploratory.

In TP1 individuals, only the combination of sTNFR1 plasma levels and CCR2 and CXCR4 expression on PMN-MDSCs was significantly associated with NC score (Table 3) (p-values corrected for multiple comparisons: sTNFR1 = 0.0109, CXCR4 = 0.0366, CCR2 = 0.0361) and both AVLT delayed scores (corrected p-values for the AVLT Delayed Rec. Post-inf.: sTNFR1 = 0.0067, CCR2 = 0.0006, CXCR4 = 0.0069 and for AVLT Delayed Rec.

TABLE 3 Multivariate regression analysis using generalized linear models (GAMs) for immunological signatures and cognitive function scores.

	Imm. signature	NC_score	Digit span total
TP1	sTNFR1/CXCR4/CCR2	**70.8% (0.0097/0.0088/0.0192)**	12.5% (0.591/0.899/0.771)
TP2	IL-3/CXCL12/SCF	**58.2% (0.0274/0.0123/0.0227)**	17.9% (**0.0876**/0.2103/0.2752)
	Imm. Signature	AVLT Delayed Rec. Post-inf.	Digit Span Forw.
TP1	sTNFR1/CXCR4/CCR2	**66.7% (0.0083/0.0063/0.0002)**	1.17% (0.879/0.761/0.839)
TP2	IL-3/CXCL12/SCF	11.5% (0.655/0.380/0.498)	11.2% (0.166/0.404/0.394)
	Imm. Signature	AVLT Delayed Rec. after 30min	Digit Span Backw.
TP1	sTNFR1/CXCR4/CCR2	**55% (0.0023/0.0052/0.0212)**	24.1% (0.444/0.507/0.956)
TP2	IL-3/CXCL12/SCF	11% (0.465/0.268/0.880)	20.1% (0.2499/**0.0773**/0.1516)
	Imm. Signature	TMT Part A	TMT Part B
TP1	sTNFR1/CXCR4/CCR2	66.4% (0.8314/0.6249/**0.0179**)	23.3% (0.107/0.352/0.350)
TP2	IL-3/CXCL12/SCF	34.2% (0.1392/**0.0436**/0.2987)	20.9% (0.1116/**0.0844**/0.1982)

Values are presented as the percentage of data deviance explained by the generalized additive model (GAM), followed by the p-values for each predictor included in the model (in the order listed in the column named Imm. Signature).
Bold letters indicate statistically significant associations between all components of the regression predictors, with the tested clinical variable.

Post-inf. after 30min: sTNFR1 = 0.0069, CCR2 = 0.0078, CXCR4 = 0.0212). In TP1 the model showed a predictor-to-sample ratio of 7.00 (3 smooth predictors), a substantial non-linear complexity for sTNFR1 and an important concurvity between CCR2 and CXCR4. The combination of sTNFR1/CCR2/CXCR4 showed also a trend to associate with OC_F in TP1, but not with the AVLT immediate recall score, or any other cognitive test scores, hence these results were not considered for multiple comparison filtering or further analysis. These results, suggested an association between immune dysregulation and delayed recall of information, memory retrieval and potentially working memory. Among the significant model-fitted associations, the NC score showed the strongest fitting (Table 3, Figure 4E), indicating that this immune signature may associate with overall post-COVID-19 symptom burden. No other trends between immunological signatures and cognitive tests were observed in the individuals of each time point. However, the limited sample size in PASC-TP1 (n=5) cohort imposed a severe limitation in the abovementioned results because of increased risk of model overfitting. We performed diagnostic assessment of the fit, overfitting, and stability of the model, including basis dimension checks, residual diagnostics, concurvity analysis, and evaluation of effective degrees of freedom (EDF). The model explained a substantial proportion of variance in NC_score (deviance explained = 70.5%; R^2_adj = 0.585). Smooth term analysis indicated a dominant nonlinear contribution of sTNFR1 (EDF = 3.82, p = 0.0036), with CXCR4 (EDF = 1.10, p = 0.037) and CCR2 (EDF = 1.00, p = 0.030) contributing more linear effects. Model diagnostics confirmed adequate basis dimensions and good model fit, with no evidence of overfitting. Concurvity analysis indicated strong redundancy between CXCR4 and CCR2 (> 0.9), while sTNFR1 showed more independent variation (0.62), suggesting that while sTNFR1 exerts an independent effect on the data, CXCR4 and CCR2 likely reflect a shared effect, rather than independent ones. Despite these diagnostic checks, the results for TP1 represent preliminary, exploratory observations because of the limited sample size and need to be validated in independent cohorts with larger sample size.

In TP2 individuals, a different signature—comprising plasma levels of IL-3, CXCL12, and SCF—showed a significant non-linear association with their NC score (Table 3, Figure 4F). The GAM was applied with the same k and penalty parameters and showed a predictor-to-sample ratio of 7.67 (3 smooth predictors). The smoothing parameters CXCL12 and SDF were shrunken towards linear effects, however, IL-3 showed a non-linear trend. Overall, these results confirmed that the penalization prevented spurious overfitting while capturing essential biological relationships. Although there were trends toward associations with memory for digit span test (OC) and TMT scores, these did not reach statistical significance. The NC score consistently showed the strongest associations with immune markers, suggesting that the subjective symptom burden aligns with measurable immunological dysregulation evident at 18 months and at 36 months after COVID-19. In this time point, the model explained a substantial proportion of variance in NC_score (deviance explained = 67.7%; R^2_adj = 0.525). Smooth term analysis showed a moderate nonlinear effect of IL3 (EDF = 3.07, p = 0.014) and CXCL12 (EDF = 1.81, p = 0.015), while SCF showed a borderline association (EDF = 2.040, p = 0.053). Multiple comparison correction validated that the results were not false positives. Model diagnostics confirmed again adequate model stability and no signs of overfitting. Concurvity analysis indicated moderate-to-high redundancy among variables, particularly between SCF and IL3 (> 0.9), suggesting again a shared underlying contribution rather than distinct effects.

Overall, GAM diagnostics for each time point showed no evidence of overfitting, with well-controlled model complexity and adequate basis dimensions. Although both models showed substantial explanatory power, concurvity indicated that more than one marker in each case reflect overlapping biological signals rather than fully independent effects, thus being of limited additional informative value. Overall, these results are hypothesis generating rather than predictive. We then visualized the fitted NC scores (presented as colored gradients going from dark blue to yellow as the score increases), for each pair of signature variables in

each of the TP1 and TP2 cohorts. These plots revealed potential "windows" (yellow areas of the plot map) in which specific immunological profiles may associate with higher NC scores (reflected by green/yellow areas in the heatmaps), corresponding to worse clinical status for the cohort of each time point (Figures 4E, F).

4 Discussion

Reliable biomarkers of PASC are lacking, making the detection process lengthy and imprecise. Given that up to 35% of PASC individuals experience cognitive phenotypes (4–7), identifying links between prolonged immune dysregulation, neuroinflammation, and PASC-related cognitive impairment could support development of tools for managing PASC and stratifying those at risk. Here, we investigated whether long-term alterations in neutrophil phenotypes and systemic immune mediators are linked to cognitive dysfunction in individuals self-reporting issues with COVID-19 linked to PASC. We demonstrate persisting cognitive deficits and sustained remodeling of neutrophil maturation at 18 and 36 months after COVID-19, closely associated with each other in individuals reporting PASC, providing a previously unknown immuno-cognitive interconnection. Although the classification of patients solely according to their self-reported recovery status may introduce some degree of classification bias, since cognitive impairment could influence self-awareness and recall, this approach reflects the current clinical practice. Currently, no validated objective biomarkers or diagnostic tests exist to diagnose PASC and stratify patients at risk. Consequently, patient-reported persistence of symptoms remains the primary criterion to identify patients with PASC. Although diverging medical histories, potential racial heterogeneity, life conditions/education levels, underlying conditions or other non-recorded comorbidities or parameters might pose a limitation to these findings, importantly, our cognition-related findings resulted from standardized objective cognitive assessments, rather than self-reported deficits, thus reducing the likelihood of common-method bias. Future studies incorporating longitudinal clinical evaluations and emerging objective biomarkers of PASC are needed to further improve cohort classification and fully address potential misclassification bias.

Aberrant neutrophil activation is a well-established contributor to acute COVID-19 severity, as well as to long-term persistent inflammation and tissue damage (18–21). Data on long-term neutrophil dynamics in PASC, however, are scarce. Our findings extend the known time frame of neutrophil alterations and provide new evidence of specific neutrophil subset changes that persist for more than 18 months following COVID-19. Although elevated neutrophil numbers during inflammation, has been hypothesized to contribute to cognitive dysfunction post-COVID-19, there have been no significant associations between neutrophils and cognitive symptoms at 18 months so far (61). To our knowledge, this is the first evidence suggesting neutrophil remodelling in PASC in individuals recruited at 19–36 months and supporting that this remodeling, related to immature neutrophils, aligns with the mental, neurological, and physical symptoms experienced by COVID-19 survivors.

In contrast to earlier findings from 3–6 months post-infection—which describe expansion of immature neutrophil subsets (18, 21, 22)—we observed an expansion of active and degranulating $CD16^{+}CD62L^{low}$ neutrophils at the expense of the $CD16^{-}CD62L^{-}$ immature subset at the 18-month time point. This could result from accelerated maturation and activation, following neutrophil bone marrow release (62). Alternatively, reduced production or dysregulated egress of immature neutrophils may be accompanied by prolonged circulation of mature neutrophils. Both scenarios reflect functional shifts and potential chronic stimulation (e.g., low-grade inflammation), resulting in stable neutrophil counts but altered population composition. This could also reflect long-term shifts in inflammatory homeostasis or epigenetic training at the level of hematopoietic stem cells in individuals with PASC. Indeed, similar trained phenotypes have been described for neutrophils after BCG vaccination (63) and more recently in monocytes from COVID-19 patients compared to healthy controls (24). These observations require further validation in larger cohorts, since the relatively small sample size—particularly in the PASC-TP1 group—may limit the robustness and generalizability of our findings. Additionally, the 18-month cutoff, although suitable for this study, doesn't represent a biologically or clinically discrete boundary between two fundamentally different post-COVID-19 phases. Subsequent literature has extended beyond the 18-month timeframe and this predefined threshold represents a limitation of the study design. Despite the above, our results support the idea that the primary distinction between PASC and REC individuals lies in neutrophil production and maturation, rather than in the presence of an acute activation signal.

Immature neutrophil subsets—particularly PMN-MDSCs—can distinguish mild from severe COVID-19, correlate with C-reactive protein and lactate levels, and even predict fatal outcomes (25, 58, 59). Moreover, persistent PMN-MDSC expansion has been associated with long-term immunosuppressive phenotypes (21, 25, 53). By contrast, our data derived from unbiased high-dimensional clustering, confirmed with independent manual gating, reveal a reduction of PMN-MDSC–like neutrophils 18 months after COVID-19 in PASC individuals with self-reported cognitive impairment, with the frequency of these being higher in the PASC-TP2 cohort (19–36 months after COVID-19) compared to the PASC-TP1 cohort. To our knowledge, no previous studies have applied unsupervised clustering to neutrophils beyond 6 months post-COVID-19. This could reflect ongoing low-grade inflammation, similar to the acute phase (64), or sustained activation of emergency granulopoiesis during the first 6 months post-infection (21, 22, 65). However, because of the cross-sectional nature of this study, limiting causal interpretation capacity, further validation would be necessary to address to above hypotheses. We further identify $CXCR4^{+}TREM\text{-}1^{+}CCR2^{+}$ PMN-MDSCs as a dominant neutrophil subset in both TP1 and TP2 REC and PASC cohorts, representing a novel PMN-MDSC signature in PASC. Because CCR2 and CXCR4 are involved in neutrophil maturation and egress or retention within the bone marrow or inflamed tissues (56, 57), these findings suggest impairment in these regulatory processes, rather than a return to baseline haematopoiesis. The identified PASC-TP1-related signature (increased CXCR4, TREM-1, CCR2) might be indicative of enhanced homing to tissues or the

bone marrow (56). On the other hand, the PASC-TP2-related signature (increased CD11b, CD336, and CD62L) might suggest enhanced mobilization from the bone marrow and partial neutrophil activation (via CD62L), possibly reflecting resolution of inflammation. Importantly, CXCR4 and CCR2, along with CD16 are expressed at distinct stages of neutrophil maturation when, during granulopoiesis, neutrophil progenitors entering circulation exhibit lower CXCR4 and higher CD62L. CXCR4, in particular, is associated with maturation and clearance of aged neutrophils (56, 57). Thus, our findings, although exploratory, might link altered neutrophil life cycle dynamics—including reduced maturation and premature differentiation—to PASC.

Emergency hematopoiesis is a hallmark of acute COVID-19 severity, characterized by leukocytosis, neutrophil predominance, neutrophil hyperactivation, and heightened PMN-MDSC activity (66). Phenotypic markers of this response, such as low-density granulocytes in various maturation states, can be detected in peripheral blood during acute infection (67). While PMN-MDSCs typically expand during acute infection and remain elevated for up to 3 months post-COVID-19, this delayed depletion at TP1 suggests incomplete resolution of inflammation or suppressed immunoregulatory pathways and may contribute to chronic low-grade inflammation in PASC individuals. Additionally, the lack of difference between REC and PASC PMN-MDSCs, in the TP2 individuals, might granulopoietic remodeling in both the TP1 cohort and the TP2 cohorts. At the same time, individuals with PASC in the cohort recruited in TP2 (19–36 months after COVID-19), showed alterations in CXCL12, IL-3, and IL-6—factors associated with emergency granulopoiesis. These changes were not evident in the individuals of TP2, suggesting partial resolution of immune dysregulation, rather than a chronic unresolved phenotype. This finding is consistent with prior observations of inflammation resolution by year 2 and the presence of epigenetic changes in circulating hematopoietic stem and progenitor cells up to 12 months after severe COVID-19 (24). Together, our findings are consistent with the hypothesis that dysregulated granulopoiesis may contribute to altered neutrophil composition, and could be associated with systemic effects such as persistent inflammation or cognitive dysfunction in PASC. Still, the modest persistence of these alterations even at 36 months may warrant further exploration of emergency granulopoiesis and its possible links to cognitive dysfunction in PASC. Even though direct such links have not yet been uncovered, emergency granulopoiesis, via cytokine or ROS infiltration to CNS could exacerbate microglial activation (68), and predispose to cognitive dysfunction.

There is also a growing evidence base supporting a connection between immune dysregulation and COVID-19-associated neuroinflammation (12, 16). Microglial loss or overactivation, IL-1 and IL-6–mediated vascular inflammation, and neutrophil granule deposition in fatal cases have all been reported (9). These processes are partly driven by elevated IFN, IL-1, and IL-6, as well as neutrophil proteases and NETs, which can disrupt BBB integrity (9, 17, 18). Concurrently, neuroinflammatory markers in the hippocampus and frontal cortex, along with plasma biomarkers of neuropathogenesis, correlate with persistent cognitive symptoms during the transition from acute COVID-19 to PASC (69, 70). In our cohort, individuals with PASC defined by cognitive deficits, exhibited episodic memory and executive function impairments up to 36 months post-infection, extending prior analyses that focused on the 3–12 month window (71). By examining systemic and neutrophil-specific changes together, we identify a novel and robust association between PMN-MDSC/neutrophil maturation signatures and cognitive scores. Interestingly, findings regarding neutrophil subsets and functional alterations were present also in the TP2 cohort, suggesting that the total number of neutrophils and neutrophil immature or functionally discrete subsets, is not resolved even at 36 months after COVID-19. This could partially justify the persistence of cognitive symptoms. However, as the observed changes in TP2 are fewer, the persistence of cognitive symptoms might reflect changes in other immune compartments as well, such as T-cells, which are affected by the presence of PMN-MDSCs but also play a role in PASC (25, 45). Further studies are required to shed more light into this notion. Additionally, these associations do not establish causality or provide information on the progression and trajectory of PASC, and thus future longitudinal studies incorporating serial neuroimaging and neurodegenerative biomarkers are needed to determine whether persistent inflammation in PASC confers an elevated risk of long-term cognitive decline or neurodegeneration. The potential presence of additional comorbidities or other parameters (diverging medical histories, race, underlying comorbidities, life conditions/education levels) that were not assessed or detected in our cohort at the time of recruitment, also imposes some homogeneity limitations in this study. Finally, the limited sample size in PASC-TP1 imposes a severe limitation and makes the TP1 results preliminary, exploratory observations, that need to be validated in independent cohorts and with much larger sample size. However, our overall findings support the hypothesis that peripheral myeloid dysregulation is linked to CNS processes and pathogenesis and that prolonged dysregulation may impair adult neurogenesis and learning [12]. To date, neutrophil-associated immune signatures like NET markers, increased chemokines, and proteases have mostly been linked to the pulmonary sequelae of PASC (72) rather than the cognitive outcomes, as we show here. Several of the soluble factors identified in our study—including sTNFR1, sTNFR2, CCL2, and IL-3—have also been implicated in neurodegenerative disorders and pre-dementia states (73–80). Although the precise impact mechanisms are not yet elucidated, direct connections between sTNFRs and Alzheimer's disease have been uncovered, with TNFR1 deletion reducing and TNFR2 deletion exacerbating the disease, suggesting these receptors have opposing functions in brain health (81). Furthermore, IL-3 has additionally been associated with COVID-19 severity and mortality (82). Although PASC and classical neurodegenerative diseases differ in clinical trajectory, their shared immunological features raise important questions about long-term neurodegenerative risk in PASC populations.

In summary, our exploratory findings suggest that impaired granulopoiesis and neutrophil maturation—both at 18 months and at 36 months COVID-19— might be associated with overall symptom burden and cognitive deficits in PASC. Our study is limited by the small sample size of PASC-TP1 and is a cross-sectional, hypothesis generating study, that pinpoints long-term alterations in immature neutrophil immune signatures and systemic granulopoiesis -related factor levels as potential drivers of PASC-related cognitive impairment. By exploring the connection between systemic immune dysregulation with neuropsychological

outcomes, this study suggests new perspectives for the clinical understanding and management of cognitive dysfunction in PASC.

Data availability statement

The data that support the findings of this study are available on request to the corresponding author. Part of the data is not publicly available due to privacy or ethical restrictions.

Ethics statement

The studies involving humans were approved by Ethics Committee of the Faculty of Medicine, Masaryk University (approval no. 76/2022). The studies were conducted in accordance with the local legislation and institutional requirements. The participants provided their written informed consent to participate in this study.

Author contributions

IP: Conceptualization, Data curation, Methodology, Visualization, Writing – original draft, Investigation, Writing – review & editing. PL: Data curation, Investigation, Methodology, Writing – review & editing. TF: Data curation, Writing – review & editing. GB: Data curation, Methodology, Writing – review & editing. KK: Data curation, Writing – review & editing. MS: Investigation, Writing – review & editing. MJ: Methodology, Writing – review & editing. FK: Methodology, Writing – review & editing. PK: Supervision, Writing – review & editing. LV: Data curation, Methodology, Writing – review & editing. MR: Investigation, Methodology, Writing – review & editing. PB: Data curation, Methodology, Writing – review & editing. DU: Data curation, Methodology, Writing – review & editing. IR: Investigation, Supervision, Writing – review & editing. MH: Investigation, Methodology, Supervision, Writing – review & editing. EB: Data curation, Investigation, Methodology, Writing – review & editing. JF: Conceptualization, Investigation, Methodology, Supervision, Writing – review & editing.

Funding

The author(s) declared that financial support was received for this work and/or its publication. This work was supported by the Ministry of Health of the Czech Republic in cooperation with the Czech Health Research Council within the National Institute for Neurology Research, project No. NW26A-NEURIN, and by the Ministry of Education, Youth and Sports (MEYS), Czech National Node to the European Clinical Research Infrastructure Network (CZECRIN, LM2023049) and project no. LX22NPO5107 (MEYS), financed by the European Union – Next Generation EU. This project has also received funding from the European Union's Horizon Europe research and innovation programme under grant agreement No. 101137484 (BEATsep). Additional support was provided by the Development of Research Organization (DRO) program, Institute of Hematology and Blood Transfusion – UHKT (00023736) and Faculty Hospital Brno - FNB (65269705) from the the Ministry of Health of the Czech Republic.by the European Union—project EATRIS-CZ (reg. no. CZ.02.01.01/00/23_015/0008208).

Acknowledgments

The authors would like to thank the technical staff of the Center for Translational Medicine, St. Anne's University Hospital in Brno and the Faculty of Medicine, Masaryk University, for their support. They also acknowledge the core facility MAFIL, supported by MEYS CR (LM2023050 Czech-BioImaging), which is part of the Euro-BioImaging (www.eurobioimaging.eu). Advanced Light Microscopy and Medical Imaging Node (Brno, CZ). Finally, the authors would like to thank Dr. Jessica Tamanini of Insight Editing London for editing the manuscript prior to submission.

Conflict of interest

The author(s) declared that this work was conducted in the absence of any commercial or financial relationships that could be construed as a potential conflict of interest.

Generative AI statement

The author(s) declared that generative AI was not used in the creation of this manuscript.

Any alternative text (alt text) provided alongside figures in this article has been generated by Frontiers with the support of artificial intelligence and reasonable efforts have been made to ensure accuracy, including review by the authors wherever possible. If you identify any issues, please contact us.

Publisher's note

All claims expressed in this article are solely those of the authors and do not necessarily represent those of their affiliated organizations, or those of the publisher, the editors and the reviewers. Any product that may be evaluated in this article, or claim that may be made by its manufacturer, is not guaranteed or endorsed by the publisher.

Supplementary material

The Supplementary Material for this article can be found online at: https://www.frontiersin.org/articles/10.3389/fimmu.2026.1885356/full#supplementary-material

References

1. Antonelli M, Pujol JC, Spector TD, Ourselin S, Steves CJ. Risk of long COVID associated with delta versus omicron variants of SARS-CoV-2. *Lancet*. (2022) 399:2263–4. doi: 10.1016/S0140-6736(22)00941-2

2. Chen C, Haupert SR, Zimmermann L, Shi X, Fritsche LG, Mukherjee B. Global prevalence of post-coronavirus disease 2019 (COVID-19) condition or long COVID: A meta-analysis and systematic review. *J Infect Dis*. (2022) 226:1593–607. doi: 10.1093/infdis/jiac136

3. Chen Z, Azman AS, Chen X, Zou J, Tian Y, Sun R, et al. Global landscape of SARS-CoV-2 genomic surveillance and data sharing. *Nat Genet*. (2022) 54:499–507. doi: 10.1038/s41588-022-01033-y

4. Ceban F, Ling S, Lui LMW, Lee Y, Gill H, Teopiz KM, et al. Fatigue and cognitive impairment in post-COVID-19 syndrome: A systematic review and meta-analysis. *Brain Behavior Immun*. (2022) 101:93–135. doi: 10.1016/j.bbi.2021.12.020

5. Fanshawe JB, Sargent BF, Badenoch JB, Saini A, Watson CJ, Pokrovskaya A, et al. Cognitive domains affected post-COVID-19; a systematic review and meta-analysis. *Euro J Neurol*. (2025) 32(1):e16181. doi: 10.1111/ene.16181

6. Elboraay T, Ebada MA, Elsayed M, Aboeldahab HA, Salamah HM, Rageh O, et al. Long-term neurological and cognitive impact of COVID-19: a systematic review and meta-analysis in over 4 million patients. *BMC Neurol*. (2025) 25:250. doi: 10.1186/s12883-025-04174-9

7. Knight DRT, Munipalli B, Logvinov II, Halkar MG, Mitri G, Dabrh AMA, et al. Perception, prevalence, and prediction of severe infection and post-acute sequelae of COVID-19. *Am J Med Sci*. (2022) 363:295–304. doi: 10.1016/j.amjms.2022.01.002

8. Peluso MJ, Deeks SG. Mechanisms of long COVID and the path toward therapeutics. *Cell*. (2024) 187:5500–29. doi: 10.1016/j.cell.2024.07.054

9. Fekete R, Simats A, Bíró E, Pósfai B, Cserép C, Schwarcz AD, et al. Microglia dysfunction, neurovascular inflammation and focal neuropathologies are linked to IL-1- and IL-6-related systemic inflammation in COVID-19. *Nat Neurosci*. (2025) 28:558–76. doi: 10.1038/s41593-025-01871-z

10. Fernández-Castañeda A, Lu P, Geraghty AC, Song E, Lee M-H, Wood J, et al. Mild respiratory COVID can cause multi-lineage neural cell and myelin dysregulation. *Cell*. (2022) 185:2452–2468.e16. doi: 10.1016/j.cell.2022.06.008

11. Rua C, Raman B, Rodgers CT, Newcombe VFJ, Manktelow A, Chatfield DA, et al. Quantitative susceptibility mapping at 7 T in COVID-19: brainstem effects and outcome associations. *Brain*. (2024) 147:4121–30. doi: 10.1093/brain/awae215

12. Wynberg E, Han AX, Van Willigen HDG, Verveen A, Van Pul L, Maurer I, et al. Inflammatory profiles are associated with long COVID up to 6 months after COVID-19 onset: A prospective cohort study of individuals with mild to critical COVID-19. *PloS One*. (2024) 19:e0304990. doi: 10.1371/journal.pone.0304990

13. VanElzakker MB, Bues HF, Brusaferri L, Kim M, Saadi D, Ratai E-M, et al. Neuroinflammation in post-acute sequelae of COVID-19 (PASC) as assessed by [11C] PBR28 PET correlates with vascular disease measures. *Brain Behavior Immun*. (2024) 119:713–23. doi: 10.1016/j.bbi.2024.04.015

14. Horowitz T, Dudouet P, Campion J-Y, Kaphan E, Radulesco T, Gonzalez S, et al. Persistent brain metabolic impairment in long COVID patients with persistent clinical symptoms: a nine-month follow-up [18F]FDG-PET study. *Eur J Nucl Med Mol Imaging*. (2024) 51:3215–22. doi: 10.1007/s00259-024-06775-x

15. Martini AL, Carli G, Caminiti SP, Kiferle L, Leo A, Perani D, et al. Persistent dysfunctions of brain metabolic connectivity in long-covid with cognitive symptoms. *Eur J Nucl Med Mol Imaging*. (2025) 52:810–22. doi: 10.1007/s00259-024-06937-x

16. Talla A, Vasaikar SV, Szeto GL, Lemos MP, Czartoski JL, MacMillan H, et al. Persistent serum protein signatures define an inflammatory subcategory of long COVID. *Nat Commun*. (2023) 14:3417. doi: 10.1038/s41467-023-38682-4

17. Vanderheiden A, Klein RS. Neuroinflammation and COVID-19. *Curr Opin Neurobiol*. (2022) 76:102608. doi: 10.1016/j.conb.2022.102608

18. Shafqat A, Omer MH, Albalkhi I, Alabdul Razzak G, Abdulkader H, Abdul Rab S, et al. Neutrophil extracellular traps and long COVID. *Front Immunol*. (2023) 14:1254310. doi: 10.3389/fimmu.2023.1254310

19. Hafkamp FMJ, Taanman-Kueter EWM, Van Capel TMM, Wynberg E, Van Willigen HDG, Verveen A, et al. Aberrant neutrophil degranulation in hospitalized patients with COVID-19 partially remains for 6 months. *Eur J Immunol*. (2024) 54:2350404. doi: 10.1002/eji.202350404

20. Thierry AR, Salmon D. Inflammation-, immunothrombosis,- and autoimmune-feedback loops may lead to persistent neutrophil self-stimulation in long COVID. *J Med Virol*. (2024) 96:e29887. doi: 10.1002/jmv.29887

21. Siemińska I, Węglarczyk K, Surmiak M, Kurowska-Baran D, Sanak M, Siedlar M, et al. Mild and asymptomatic COVID-19 convalescents present long-term endotype of immunosuppression associated with neutrophil subsets possessing regulatory functions. *Front Immunol*. (2021) 12:748097. doi: 10.3389/fimmu.2021.748097

22. Hocini H, Wiedemann A, Blengio F, Lefebvre C, Cervantes-Gonzalez M, Foucat E, et al. Neutrophil activation and immune thrombosis profiles persist in convalescent COVID-19. *J ClinImmunol*. (2023) 43:882–93. doi: 10.1007/s10875-023-01459-x

23. De Zuani M, Frič J. Train the trainer: Hematopoietic stem cell control of trained immunity. *Front Immunol*. (2022) 13:827250. doi: 10.3389/fimmu.2022.827250

24. Cheong J-G, Ravishankar A, Sharma S, Parkhurst CN, Grassmann SA, Wingert CK, et al. Epigenetic memory of coronavirus infection in innate immune cells and their progenitors. *Cell*. (2023) 186:3882–3902.e24. doi: 10.1016/j.cell.2023.07.019

25. Sacchi A, Grassi G, Bordoni V, Lorenzini P, Cimini E, Casetti R, et al. Early expansion of myeloid-derived suppressor cells inhibits SARS-CoV-2 specific T-cell response and may predict fatal COVID-19 outcome. *Cell Death Dis*. (2020) 11:921. doi: 10.1038/s41419-020-03125-1

26. Grassi G, Notari S, Gili S, Bordoni V, Casetti R, Cimini E, et al. Myeloid-derived suppressor cells in COVID-19: The paradox of good. *Front Immunol*. (2022) 13:842949. doi: 10.3389/fimmu.2022.842949

27. Barker-Davies RM, O'Sullivan O, Holdsworth DA, Ladlow P, Houston A, Chamley R, et al. How long is long-COVID? Symptomatic improvement between 12 and 18 months in a prospective cohort study. *BMJ Mil Health*. (2025) 171:126–33. doi: 10.1136/military-2023-002500

28. Ranucci M, Baryshnikova E, Anguissola M, Pugliese S, Ranucci L, Falco M, et al. The very long COVID: Persistence of symptoms after 12–18 months from the onset of infection and hospitalization. *JCM*. (2023) 12:1915. doi: 10.3390/jcm12051915

29. Zhang X, Lv L, Min G, Wang Q, Zhao Y, Li Y. Overview of the complex figure test and its clinical application in neuropsychiatric disorders, including copying and recall. *Front Neurol*. (2021) 12:680474. doi: 10.3389/fneur.2021.680474

30. Borkowski JG, Benton AL, Spreen O. Word fluency and brain damage. *Neuropsychologia*. (1967) 5:135–40. doi: 10.1016/0028-3932(67)90015-2

31. Schmidt M. *Rey Auditory Verbal Learning Test: A Handbook*. Los Angeles, CA: Western Psychological Services (or WPS) (1996).

32. Benedict RHB, Schretlen D, Groninger L, Dobraski M, Shpritz B. Revision of the brief visuospatial memory test: Studies of normal performance, reliability, and validity. *psychol Assess*. (1996) 8:145–53. doi: 10.1037/1040-3590.8.2.145

33. Wechsler D. *Wais-Iv Uk. 4th ed*. London: Pearson (2010). p. 1.

34. Reitan RM. Validity of the trail making test as an indicator of organic brain damage. *Percept Mot Skills*. (1958) 8:271–6. doi: 10.2466/pms.1958.8.3.271

35. White T, S RA. NAB: Neuropsychological Assessment Battery—Psychometric & Technical Manual. Lutz, FL: Psychological Assessment Resources Inc. (2003).

36. Broadbent DE, Cooper PF, FitzGerald P, Parkes KR. The cognitive failures questionnaire (CFQ) and its correlates. *Br J Clinic Psychol*. (1982) 21:1–16. doi: 10.1111/j.2044-8260.1982.tb01421.x

37. Emmaneel A, Quintelier K, Sichien D, Rybakowska P, Marañón C, Alarcón-Riquelme ME, et al. PeacoQC: Peak-based selection of high quality cytometry data. *Cytometry Pt A*. (2022) 101:325–38. doi: 10.1002/cyto.a.24501

38. Van Gassen S, Gaudilliere B, Angst MS, Saeys Y, Aghaeepour N. CytoNorm: A normalization algorithm for cytometry data. *Cytometry Pt A*. (2020) 97:268–78. doi: 10.1002/cyto.a.23904

39. Van Gassen S, Callebaut B, Van Helden MJ, Lambrecht BN, Demeester P, Dhaene T, et al. FlowSOM: Using self-organizing maps for visualization and interpretation of cytometry data. *Cytometry Pt A*. (2015) 87:636–45. doi: 10.1002/cyto.a.22625

40. Lê S, Josse J, Husson F. FactoMineR: An *R* package for multivariate analysis. *J Stat Soft*. (2008) 25(8):1–18. doi: 10.18637/jss.v025.i01

41. Ho DE, Imai K, King G, Stuart EA. MatchIt: Nonparametric preprocessing for parametric causal inference. *J Stat Soft*. (2011) 42(8):1–28. doi: 10.18637/jss.v042.i08

42. Hansen BB, Klopfer SO. Optimal full matching and related designs via network flows. *J Comput Graphical Stat*. (2006) 15:609–27. doi: 10.1198/106186006X137047

43. Rohart F, Gautier B, Singh A, Lê Cao K-A. mixOmics: An R package for 'omics feature selection and multiple data integration. *PloS Comput Biol*. (2017) 13:e1005752. doi: 10.1371/journal.pcbi.1005752

44. Wei T, Simko V. corrplot: Visualization of a correlation matrix. (2010) 0.95:. doi: 10.32614/CRAN.package.corrplot

45. Altmann DM, Whettlock EM, Liu S, Arachchillage DJ, Boyton RJ. The immunology of long COVID. *Nat Rev Immunol*. (2023) 23:618–34. doi: 10.1038/s41577-023-00904-7

46. Gallerani E, Proietto D, Dallan B, Campagnaro M, Pacifico S, Albanese V, et al. Impaired priming of SARS-CoV-2-specific naive CD8+ T cells in older subjects. *Front Immunol*. (2021) 12:693054. doi: 10.3389/fimmu.2021.693054

47. Kamp VM, Pillay J, Lammers J-W, Pickkers P, Ulfman LH, Koenderman L. Human suppressive neutrophils CD16bright/CD62Ldim exhibit decreased adhesion. *J Leukocyte Biol*. (2012) 92:1011–20. doi: 10.1189/jlb.0612273

48. Mol S, Hafkamp FMJ, Varela L, Simkhada N, Taanman-Kueter EW, Tas SW, et al. Efficient neutrophil activation requires two simultaneous activating stimuli. *IJMS*. (2021) 22:10106. doi: 10.3390/ijms221810106

49. Timmer KD, Floyd DJ, Scherer AK, Crossen AJ, Atallah J, Viens AL, et al. Multiparametric profiling of neutrophil function via a high-throughput flow cytometry-based assay. *Cells*. (2023) 12:743. doi: 10.3390/cells12050743

50. Pillay J, Kamp VM, Van Hoffen E, Visser T, Tak T, Lammers J-W, et al. A subset of neutrophils in human systemic inflammation inhibits T cell responses through Mac-1. *J Clin Invest*. (2012) 122:327–36. doi: 10.1172/JCI57990

51. Hellebrekers P, Hesselink L, Huisman A, Ten Berg M, Koenderman L, Leenen LPH, et al. Recognizing the mobilization of neutrophils with banded nuclei early after trauma. *Int J Lab Hematol*. (2020) 42(5):e224–e227. doi: 10.1111/ijlh.13272

52. Cortjens B, Ingelse SA, Calis JC, Vlaar AP, Koenderman L, Bem RA, et al. Neutrophil subset responses in infants with severe viral respiratory infection. *Clin Immunol*. (2017) 176:100–6. doi: 10.1016/j.clim.2016.12.012

53. Coudereau R, Waeckel L, Cour M, Rimmele T, Pescarmona R, Fabri A, et al. Emergence of immunosuppressive LOX-1+ PMN-MDSC in septic shock and severe COVID-19 patients with acute respiratory distress syndrome. *J Leukocyte Biol*. (2022) 111:489–96. doi: 10.1002/JLB.4COVBCR0321-129R

54. Bongers SH, Chen N, Van Grinsven E, Van Staveren S, Hassani M, Spijkerman R, et al. Kinetics of neutrophil subsets in acute, subacute, and chronic inflammation. *Front Immunol*. (2021) 12:674079. doi: 10.3389/fimmu.2021.674079

55. Van Der Pan K, De Bruin-Versteeg S, Damasceno D, Hernández-Delgado A, Van Der Sluijs-Gelling AJ, Van Den Bossche WBL, et al. Development of a standardized and validated flow cytometry approach for monitoring of innate myeloid immune cells in human blood. *Front Immunol*. (2022) 13. doi: 10.3389/fimmu.2022.935879

56. Martin C, Burdon PCE, Bridger G, Gutierrez-Ramos J-C, Williams TJ, Rankin SM. Chemokines acting via CXCR2 and CXCR4 control the release of neutrophils from the bone marrow and their return following senescence. *Immunity*. (2003) 19:583–93. doi: 10.1016/S1074-7613(03)00263-2

57. Capucetti A, Albano F, Bonecchi R. Multiple roles for chemokines in neutrophil biology. *Front Immunol*. (2020) 11:1259. doi: 10.3389/fimmu.2020.01259

58. Emsen A, Sumer S, Tulek B, Cizmecioglu H, Vatansev H, Goktepe MH, et al. Correlation of myeloid-derived suppressor cells with C-reactive protein, ferritin and lactate dehydrogenase levels in patients with severe COVID-19. *Scand J Immunol*. (2022) 95:e13108. doi: 10.1111/sji.13108

59. Omar MA, El Hawary R, Eldash A, Sadek KM, Soliman NA, Hanna MOF, et al. Neutrophilic myeloid-derived suppressor cells and severity in SARS-CoV-2 infection. *Lab Med*. (2024) 55:153–61. doi: 10.1093/labmed/lmad050

60. Bronte V, Brandau S, Chen S-H, Colombo MP, Frey AB, Greten TF, et al. Recommendations for myeloid-derived suppressor cell nomenclature and characterization standards. *Nat Commun*. (2016) 7:12150. doi: 10.1038/ncomms12150

61. Frontera JA, Betensky RA, Pirofski L, Wisniewski T, Yoon H, Ortigoza MB. Trajectories of inflammatory markers and post–COVID-19 cognitive symptoms: A secondary analysis of the CONTAIN COVID-19 randomized trial. *Neurol Neuroimmunol Neuroinflamm*. (2024) 11(3):e200227. doi: 10.1212/nxi.0000000000200227

62. Orr Y, Wilson DP, Taylor JM, Bannon PG, Geczy C, Davenport MP, et al. A kinetic model of bone marrow neutrophil production that characterizes late phenotypic maturation. *Am J Physiol Regul Intgr Comp Physiol*. (2007) 292:R1707–16. doi: 10.1152/ajpregu.00627.2006

63. Moorlag SJCFM, Rodriguez-Rosales YA, Gillard J, Fanucchi S, Theunissen K, Novakovic B, et al. BCG vaccination induces long-term functional reprogramming of human neutrophils. *Cell Rep*. (2020) 33:108387. doi: 10.1016/j.celrep.2020.108387

64. Paudel S, Ghimire L, Jin L, Jeansonne D, Jeyaseelan S. Regulation of emergency granulopoiesis during infection. *Front Immunol*. (2022) 13:961601. doi: 10.3389/fimmu.2022.961601

65. Kwiecień I, Rutkowska E, Kulik K, Kłos K, Plewka K, Raniszewska A, et al. Neutrophil maturation, reactivity and granularity research parameters to characterize and differentiate convalescent patients from active SARS-CoV-2 infection. *Cells*. (2021) 10:2332. doi: 10.3390/cells10092332

66. Wilk AJ, Lee MJ, Wei B, Parks B, Pi R, Martínez-Colón GJ, et al. Multi-omic profiling reveals widespread dysregulation of innate immunity and hematopoiesis in COVID-19. *J Exp Med*. (2021) 218:e20210582. doi: 10.1084/jem.20210582

67. Cabrera LE, Pekkarinen PT, Alander M, Nowlan KHA, Nguyen NA, Jokiranta S, et al. Characterization of low-density granulocytes in COVID-19. *PloS Pathog*. (2021) 17:e1009721. doi: 10.1371/journal.ppat.1009721

68. Almutairi MM, Sivandzade F, Albekairi TH, Alqahtani F, Cucullo L. Neuroinflammation and its impact on the pathogenesis of COVID-19. *Front Med*. (2021) 8. doi: 10.3389/fmed.2021.745789

69. Díez-Cirarda M, Yus-Fuertes M, Sanchez-Sanchez R, Gonzalez-Rosa JJ, Gonzalez-Escamilla G, Gil-Martínez L, et al. Hippocampal subfield abnormalities and biomarkers of pathologic brain changes: from SARS-CoV-2 acute infection to post-COVID syndrome. *eBioMedicine*. (2023) 94:104711. doi: 10.1016/j.ebiom.2023.104711

70. Wood GK, Sargent BF, Ahmad Z-U-A, Tharmaratnam K, Dunai C, Egbe FN, et al. Posthospitalization COVID-19 cognitive deficits at 1 year are global and associated with elevated brain injury markers and gray matter volume reduction. *Nat Med*. (2025) 31:245–57. doi: 10.1038/s41591-024-03309-8

71. Panagea E, Messinis L, Petri MC, Liampas I, Anyfantis E, Nasios G, et al. Neurocognitive impairment in long COVID: A systematic review. *Arch Clin Neuropsychol*. (2025) 40:125–49. doi: 10.1093/arclin/acae042

72. George P, Reed A, Desai S, Devaraj A, Faiez TS, Laverty S, et al. A persistent neutrophil-associated immune signature characterises post-COVID19 pulmonary sequelae. (2022) 14(671):eabo5795. doi: 10.21203/rs.3.rs-1293175/v1

73. Scalzo P, Kümmer A, Cardoso F, Teixeira AL. Increased serum levels of soluble tumor necrosis factor-α receptor-1 in patients with Parkinson's disease. *J Neuroimmunology*. (2009) 216:122–5. doi: 10.1016/j.jneuroim.2009.08.001

74. Wang Z-B, Ma Y-H, Sun Y, Tan L, Wang H-F, Yu J-T, et al. Interleukin-3 is associated with sTREM2 and mediates the correlation between amyloid-β and tau pathology in Alzheimer's disease. *J Neuroinflamm*. (2022) 19:316. doi: 10.1186/s12974-022-02679-5

75. Gavriel Y, Rabinovich-Nikitin I, Solomon B. Inhibition of CXCR4/CXCL12 signaling: a translational perspective for Alzheimer's disease treatment. *Neural Regener Res*. (2022) 17:108. doi: 10.4103/1673-5374.314303

76. Holland J, Sheehan D, Brown S, O'Flanagan S, Savinelli S, O'Keeffe F, et al. Immune response and cognitive impairment in post-COVID syndrome: A systematic review. *Am J Med*. (2025) 138:698–711.e2. doi: 10.1016/j.amjmed.2024.09.022

77. Bernier RA, Banks SJ, Panizzon MS, Andrews MJ, Jacobs EG, Galasko DR, et al. The neuroinflammatory marker sTNFR2 relates to worse cognition and tau in women across the Alzheimer's disease spectrum. *Alz Dem Diag Ass Dis Mo*. (2022) 14:e12284. doi: 10.1002/dad2.12284

78. Duggan MR, Yang Z, Cui Y, Dark HE, Wen J, Erus G, et al. Proteomic analyses reveal plasma EFEMP1 and CXCL12 as biomarkers and determinants of neurodegeneration. *Alzheimer's Dementia*. (2024) 20:6486–505. doi: 10.1002/alz.14142

79. Salai KHT, Wu L-Y, Chong JR, Chai YL, Gyanwali B, Robert C, et al. Elevated soluble TNF-receptor 1 in the serum of predementia subjects with cerebral small vessel disease. *Biomolecules*. (2023) 13:525. doi: 10.3390/biom13030525

80. Zambrano A, Otth C, Maccioni B, Concha I. IL-3 control tau modifications and protects cortical neurons from neurodegeneration. *CAR*. (2010) 7:615–24. doi: 10.2174/156720510793499011

81. Probert L. TNF and its receptors in the CNS: The essential, the desirable and the deleterious effects. *Neuroscience*. (2015) 302:2–22. doi: 10.1016/j.neuroscience.2015.06.038

82. Bénard A, Jacobsen A, Brunner M, Krautz C, Klösch B, Swierzy I, et al. Interleukin-3 is a predictive marker for severity and outcome during SARS-CoV-2 infections. *Nat Commun*. (2021) 12:1112. doi: 10.1038/s41467-021-21310-4